

# SPLIT TWO-PERIODIC AZTEC DIAMOND

MEREDITH SHEA

ABSTRACT. Recent advancements have been made to understand the statistics of the Aztec diamond dimer model under general periodic weights [2, ?]. In this work we define a model that breaks periodicity in one direction by combining two different two-periodic weightings. We compute the correlation kernel for this Aztec diamond dimer model by extending the methods developed in [3], which utilize the Eynard-Mehta theorem and a Wiener-Hopf factorization. From a form of the correlation kernel that is suitable for asymptotics, we compute the local asymptotics of the model in the different macroscopic regions present. We prove that the local asymptotics of the model agree with the typical two-periodic model in the highest order, however the sub-leading order terms are affected.

## CONTENTS

1. Introduction	2
1.1. The Aztec Diamond and Dimer Models	2
1.2. The Split Two-Periodic Aztec Diamond	4
2. Summary of Results	6
2.1. An Integral Representation of the Correlation Kernel	7
2.2. Comparison to the Two-Periodic Aztec Diamond	9
2.3. Classification of the Macroscopic Regions	10
2.4. Asymptotic Behavior	11
3. Derivation of the Correlation Kernel	14
3.1. An Intermediate Correlation Kernel	14
3.2. Proof of Theorem 2.1 when $0 < m' \leq N/2$	15
3.3. Proof of Theorem 2.1 when $N/2 < m' < N$	19
3.4. Proof of Corollary 2.1	20
4. Local Asymptotics of the Model	22
4.1. Preliminaries of Saddle Functions	22
4.2. Asymptotics of $I_{2,2}^\alpha$	26
4.3. Asymptotics of $I_{2,1}^\alpha$	30
5. An Intermediate Correlation Kernel via a Non-Intersecting Paths Process	32
5.1. Non-Intersecting Paths Process	32
5.2. Proof of Lemma 3.1	35
6. Analysis of the Eigen-Decomposition	39
6.1. Proof of Lemma 3.6	39
6.2. Poles and Zeros of $r_{a,k,N}(w)$	40
6.3. Analysis of the $F_N$ -matrices	42
Appendix A. Explicit Statement of Coefficients	43
References	43

## 1. INTRODUCTION

**1.1. The Aztec Diamond and Dimer Models.** Over the past quarter century, planar dimer models have been an active area of study. A *dimer covering* of a graph, is a subset of the edges such that each vertex of the graph is incident to exactly one edge in the covering. A *dimer model* is a probability measure on the set of all dimer coverings. To define the measure one can assign *edge weights* to the graph. The probability of a certain covering is proportional to the product of the edge weights of the dimers contained in the covering. The ideas behind dimer models were initially introduced by Kasteleyn [16] and Temperley and Fisher [20].

Dimer models are often studied under some appropriate scaling limit. Cohn, Kenyon and Propp [10] showed that a class of uniform dimer models satisfy a variational principle and that the *height function* of the model converges, in the scaling limit, to a deterministic limit. Subsequently, Kenyon, Okounkov, and Sheffield [18] showed that there are three types of Gibbs measures that can appear in dimer model with doubly periodic edge weights. These *macroscopic regions* are classified as: frozen, rough, and smooth.<sup>1</sup> In the frozen region dimers are deterministic. In the rough region dimer correlations decay polynomially with distance, while in the smooth region dimer correlations decay exponentially with distance. Not all dimer models exhibit smooth regions, however most exhibit rough regions.

A seminal example of a dimer model is domino tilings of the *Aztec diamond* [12]. The asymptotics of the simplest case, the Aztec diamond with uniform edge weights, was studied by Jockusch, Propp and Shor in [14]. They proved that the boundary between the deterministic and non-deterministic regions forms a circle. This is known as the *Arctic Circle Theorem*. A key aspect to understanding correlations of the Aztec diamond is the fact that the model is a *determinantal point process*. One approach to computing correlations is through computing the *inverse Kasteleyn matrix*.<sup>2</sup> The inverse Kasteleyn matrix for the Aztec diamond with two-periodic weights was originally computed by Chhita and Young in [9]. Further asymptotics of this model have been studied in [8, 7, 1] among others. The two-periodic Aztec diamond is, notably, the simplest Aztec diamond model which exhibits all three macroscopic regions.

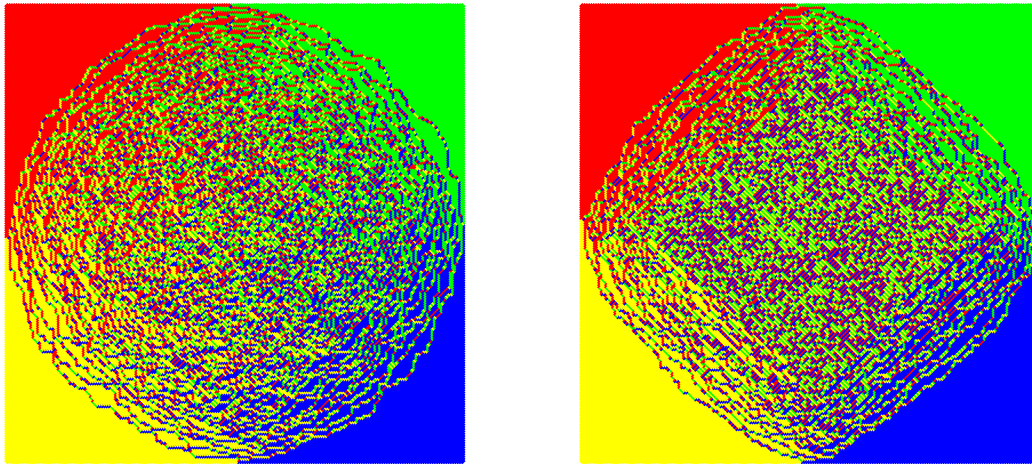


FIGURE 1. On the left is a simulation of the Aztec diamond with uniform weights. On the right is a simulation of the Aztec diamond with two periodic weights. Original code for simulation was provided by Sunil Chhita.

<sup>1</sup>In the literature these regions are also referred to as solid, liquid, and gas, respectively.

<sup>2</sup>For a general introduction to dimer models via Kasteleyn theory see [17].

An alternative approach to understanding the correlations of the dimer model uses a bijection between the Aztec diamond and a non-intersecting paths model along side the Eynard-Mehta theorem [13]. The correlation kernel of the two-periodic Aztec diamond was computed using this approach by Duits and Kuijlaars [11], via *matrix valued orthogonal polynomials* and Berggren and Duits [3], via a *Wiener-Hopf factorization*. In both of these instances, the methods produced forms of the correlation kernel that are well suited for asymptotic analysis. The Wiener-Hopf method has been related to the Kasteleyn treatment in [6] and to the MVOP method in [19].

Recently, there have been many results about the Aztec diamond with more general periodic weightings, see [5, 4, 2]. Notably in [5], Boutillier and de Tilière compute the inverse Kasteleyn matrix for the Aztec diamond with Fock's weights, which are gauge equivalent to any positive weighting of the model, and study the limit shape in cases where the weights are periodic. There is less literature, however, regarding the asymptotics of weightings that are not periodic in nature, which is the main goal of this work.

In Section 1.2, we define an extension of the typical two-periodic Aztec diamond, which we refer to as the *split two-periodic Aztec diamond*. In the split two-periodic model, periodicity is broken along a line which we refer to as the *interface* of the model. A simulation of the split two-periodic Aztec diamond is shown in Figure 2. We compute the correlation kernel of this new model by extending the methods developed in [3]. The statement of the correlation kernel is found in Section 2.1. The rest of our discussion in Section 2 relates to defining the macroscopic regions and computing the local asymptotic of the model away from the boundaries and interface.

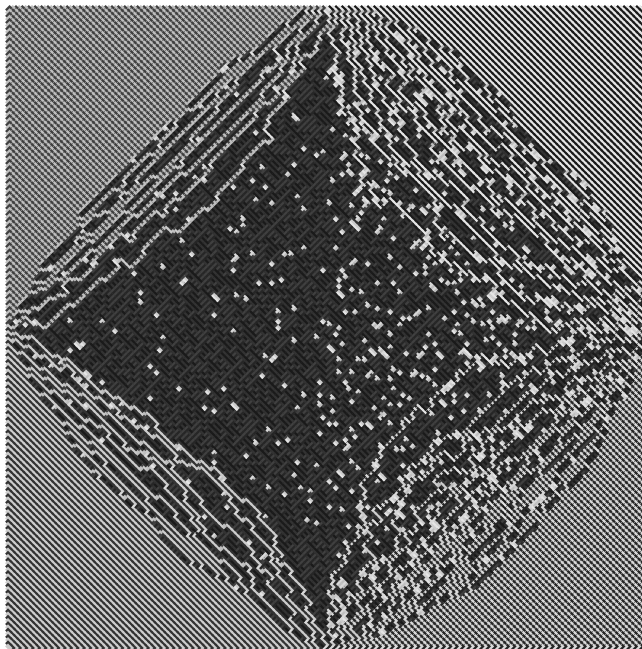


FIGURE 2. Simulated split Aztec diamond where  $N = 200$ ,  $\alpha = 1/4$ , and  $\beta = 1/2$ . The tiles are colored by an 8 color gray scale to accentuate the smooth region. Original code for simulation was provided by Sunil Chhita.

The local asymptotics illustrate how the new model maintains much of the asymptotic behavior seen in the two-periodic case. The differences between the split two-periodic model and its two-periodic counter parts are highlighted via the discussion in Section 2.4. The biggest difference in the local asymptotic behavior is seen in the decay of the sub-leading order term of the kernel in certain

parts of the smooth region of the model. Further work should be done to study the behavior of the model near and across the interface. These results suggest that where the smooth-rough boundary meets the interface behaves differently than the typical rough-smooth boundary cusp found in the two-periodic Aztec diamond.

This work also presents a prescription for deriving the correlation kernel for other non-periodic models. One can follow the work presented in Section 5 to obtain an intermediate kernel, like the one stated in Lemma 3.1, for instances when the interface is moved to the right or left in the scaled picture of the Aztec diamond. Model simulations suggest that the correlation between the two sides of the interface has more complicated behavior under these circumstances.

1.1.1. *Acknowledgements.* The author would like to thank Sunil Chhita for fruitful discussion throughout this project. Part of this research was performed while the author was visiting the Institute for Pure and Applied Mathematics (IPAM), which is supported by the National Science Foundation Grant No. DMS-1925919.

1.2. **The Split Two-Periodic Aztec Diamond.** We start by defining the vertex and edge sets of the Aztec diamond of size  $n$ . The vertices are given by,

$$(1) \quad W_n^{\text{Az}} = \{(2j + 1, 2k) : 0 \leq j \leq n - 1 \text{ and } 0 \leq k \leq n\}$$

$$(2) \quad B_n^{\text{Az}} = \{(2j, 2k + 1) : 0 \leq j \leq n \text{ and } 0 \leq k \leq n - 1\}$$

The Aztec diamond is a bipartite graph, so we write the set of all vertices as  $V_n^{\text{Az}} = W_n^{\text{Az}} \oplus B_n^{\text{Az}}$ . The edges are given by,

$$(3) \quad E_n^{\text{Az}} = \left\{ ((2j + 1, 2k), (2j + 1 \pm 1, 2k + 1)) : 0 \leq j \leq n - 1, 0 \leq k \leq n - 1 \right\} \\ \cup \left\{ ((2j + 1, 2k), (2j + 1 \pm 1, 2k - 1)) : 0 \leq j \leq n - 1, 1 \leq k \leq n \right\}$$

Examples of the Aztec diamond graph are given in Figure 3. For the split two-periodic Aztec

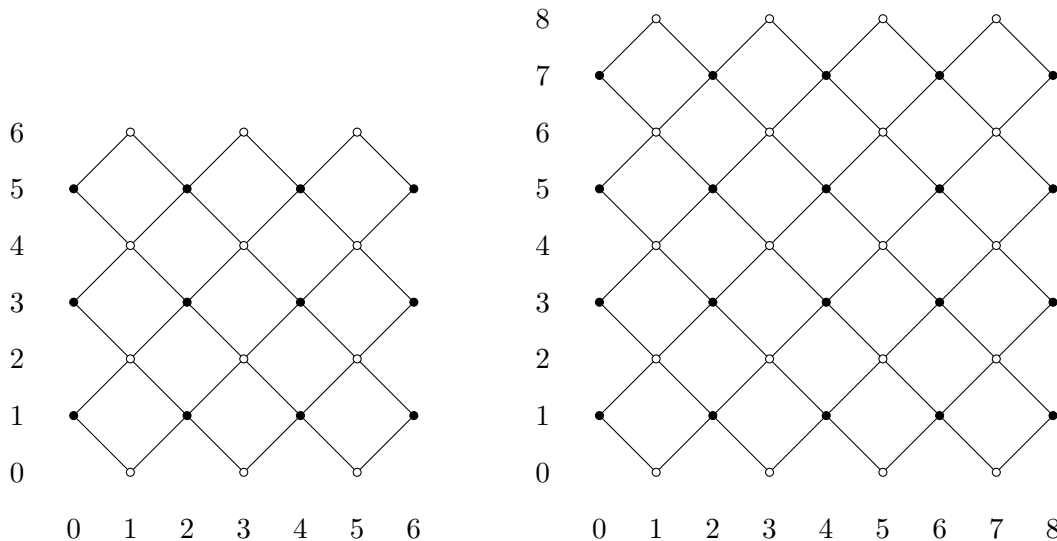


FIGURE 3. Examples of the Aztec diamond graph. On the left is the Aztec diamond of size  $n = 3$ , on the right is the Aztec diamond of size  $n = 4$ .

diamond we will assume that  $n$  is even, so we write  $n = 2N$ . Now we are ready to define the

weights of the split two-periodic Aztec diamond. Let  $b = (b_x, b_y) \in \mathbf{B}$  and  $w = (w_x, w_y) \in \mathbf{W}$ . We say that  $b$  and  $w$  are neighbors if there is an edge between the two vertices. If this is the case we write  $b \sim w$ . We will use the notation  $\text{wt}(b, w)$  to denote the weight of the edge connecting the vertices  $b$  and  $w$ . Note that  $\text{wt}(b, w) = \text{wt}(w, b)$ . The weight function for the split two-period Aztec diamond is,

$$(4) \quad \text{wt}(b, w) = \begin{cases} \alpha^2 & \text{if } w_x \equiv 1 \pmod{4}, w_y \equiv 0 \pmod{4}, w - b = (\pm 1, -1), \text{ and } w_x < 2N \\ \alpha^{-2} & \text{if } w_x \equiv 1 \pmod{4}, w_y \equiv 2 \pmod{4}, w - b = (\pm 1, -1), \text{ and } w_x < 2N \\ \beta^2 & \text{if } w_x \equiv 1 \pmod{4}, w_y \equiv 0 \pmod{4}, w - b = (\pm 1, -1), \text{ and } w_x > 2N \\ \beta^{-2} & \text{if } w_x \equiv 1 \pmod{4}, w_y \equiv 2 \pmod{4}, w - b = (\pm 1, -1), \text{ and } w_x > 2N \\ 1 & \text{if } w_x \equiv 1 \pmod{4}, \text{ and } w - b = (\pm 1, 1) \\ 1 & \text{if } w_x \equiv 3 \pmod{4}, \text{ and } w - b = (\pm 1, \pm 1) \\ 0 & \text{otherwise} \end{cases}$$

where  $0 < \alpha, \beta < 1$  are constants. The last case in the above formula indicates the the weight is 0 if the vertices are not neighbors. If  $\alpha = \beta$ , this model recovers the usual two-periodic Aztec diamond. If  $\alpha = \beta = 1$  we recover the uniform Aztec diamond, however we will generally assume that the constants are not equal to 1. The split two-periodic Aztec diamond of size  $2N = 4$  is shown in Figure 4. We will refer to the line were the weighting changes as the *interface* of the model. In this coordinate convention, the interface occurs along the vertical line  $x = 2N$ .

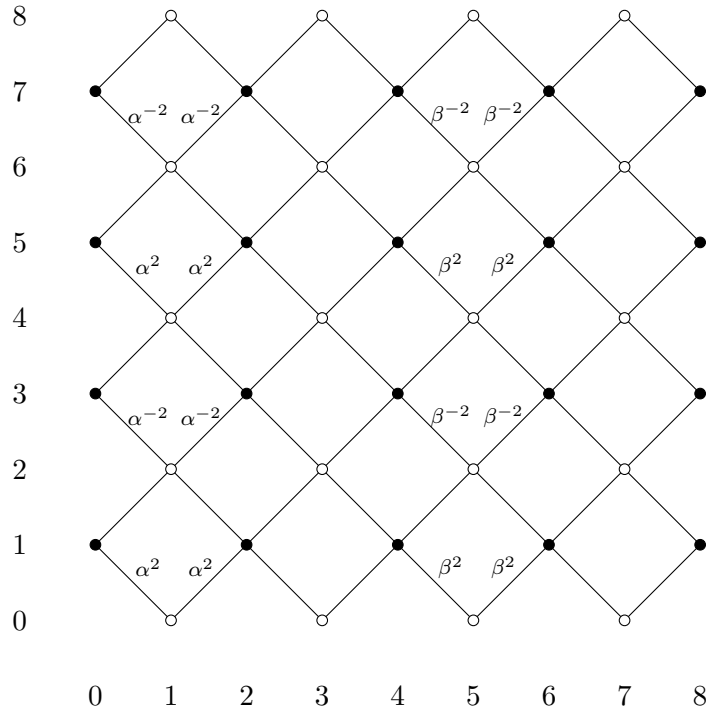


FIGURE 4. The Aztec diamond of size  $2N = 4$  with coordinates given by equations (1)-(2) and weights given by equation (4). All unlabeled edged have weight 1.

To produce the correlation kernel for the split two-periodic Aztec diamond we will extend the work of Berggren and Duits in [3]. Their work computes the correlation kernel for a class of non-intersecting paths models, which are detailed in Section 5 of this work. Their work relates the Aztec diamond to a non-intersecting paths process, which is shown to be equivalent to the Aztec

diamond model. We detail this equivalence in Section 5 of this work. For now, we make some simple changes to the coordinate convention on the Aztec diamond which will allow us to immediately relate the statement of the kernel to exact positions in the Aztec diamond. For details on why this transformation is valid, one should refer to the bijections developed in Section 5.

To transform the coordinates, we start by moving the white vertices of the Aztec diamond to be level with the row of black vertices immediately below them. Consider  $w \in \mathbb{W}$  with initial coordinate  $(2j + 1, 2k)$ , it now has the coordinate  $(2j + 1, 2k - 1)$ . Next, to any vertex  $v = (v_x, v_y)$  we make the following change to the  $y$ -coordinate,

$$v_y \mapsto \frac{1}{2}v_y - 2N - \frac{1}{2}$$

This transformation is depicted in Figure 5. For the Aztec diamond of size  $n$  the vertex sets become the following under the new coordinate convention,

$$(5) \quad \mathbb{W}_n^{\text{Az-Alt}} = \left\{ (2j + 1, k) : 0 \leq j < n \text{ and } -n - 1 \leq k \leq -1 \right\}$$

$$(6) \quad \mathbb{B}_n^{\text{Az-Alt}} = \left\{ (2j, k) : 0 \leq j < n \text{ and } -n \leq k \leq -1 \right\}$$

And the edges are now given by,

$$(7) \quad \mathbb{E}_n^{\text{Az-Alt}} = \left\{ ((2j + 1, k), (2j + 1 \pm 1, k)) : 0 \leq j < n \text{ and } -n \leq k \leq -1 \right\} \\ \cup \left\{ ((2j + 1, k), (2j + 1 \pm 1, k + 1)) : 0 \leq j < n \text{ and } -n - 1 \leq k \leq -2 \right\}$$

For the correlation kernel given in Section 2.1, these transformed coordinates will be the ones we use.

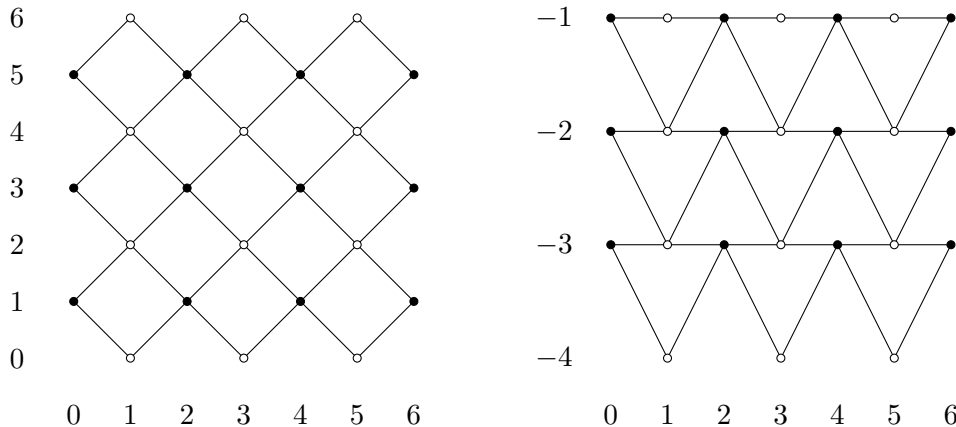


FIGURE 5. The above depicts the coordinate changes on the size 3 Aztec diamond.

## 2. SUMMARY OF RESULTS

In this section, we will detail the main results of this work. This starts with the statement of the correlation kernel of the split two-periodic Aztec diamond, which we later compute by extending the methods of Berggren and Duits [3]. We then relate this kernel to the kernel of the typical two-periodic Aztec diamond model. Lastly, we classify the macroscopic regions of the model by way of computing the local asymptotics. In particular, we emphasize the differences in the local asymptotics of the split two-periodic model compared to the typical two-periodic model.

**2.1. An Integral Representation of the Correlation Kernel.** In order to state the correlation kernel of the model, we first define some preliminary functions. We start with the matrices,

$$\begin{aligned}\phi_{\varepsilon,1}(z) &= \begin{pmatrix} 1 & \varepsilon^2 z^{-1} \\ \varepsilon^{-2} & 1 \end{pmatrix} & \phi_{\varepsilon,2}(z) &= \frac{1}{1-z^{-1}} \begin{pmatrix} 1 & \varepsilon^2 z^{-1} \\ \varepsilon^{-2} & 1 \end{pmatrix} \\ \phi_3(z) &= \begin{pmatrix} 1 & z^{-1} \\ 1 & 1 \end{pmatrix} & \phi_4(z) &= \frac{1}{1-z^{-1}} \begin{pmatrix} 1 & z^{-1} \\ 1 & 1 \end{pmatrix}\end{aligned}$$

and define

$$(8) \quad \Phi_\varepsilon(z) = \phi_{\varepsilon,1}(z)\phi_{\varepsilon,2}(z)\phi_3(z)\phi_4(z)$$

It is useful to express  $\Phi_\varepsilon(z)$  in terms of its eigen-decomposition,

$$(9) \quad \Phi_\varepsilon(z) = E_\varepsilon(z) \begin{pmatrix} r_{\varepsilon,1}(z) & 0 \\ 0 & r_{\varepsilon,2}(z) \end{pmatrix} E_\varepsilon(z)^{-1}$$

The eigenvalues of  $\Phi_\varepsilon(z)$  are explicitly,

$$(10) \quad r_{\varepsilon,1}(z) = \frac{1}{(z-1)^2} \left( (z+1)^2 + 2z(\varepsilon^2 + \varepsilon^{-2}) + 2(\varepsilon + \varepsilon^{-1})\sqrt{z^3 + (\varepsilon^2 + \varepsilon^{-2})z^2 + z} \right)$$

and

$$(11) \quad r_{\varepsilon,2}(z) = \frac{1}{(z-1)^2} \left( (z+1)^2 + 2z(\varepsilon^2 + \varepsilon^{-2}) - 2(\varepsilon + \varepsilon^{-1})\sqrt{z^3 + (\varepsilon^2 + \varepsilon^{-2})z^2 + z} \right)$$

We also define,

$$(12) \quad \begin{aligned}F_{\varepsilon,1}(z) &= E_\varepsilon(z) \begin{pmatrix} 1 & 0 \\ 0 & 0 \end{pmatrix} E_\varepsilon(z)^{-1} \\ &= \begin{pmatrix} \frac{1}{2} - \frac{z(\varepsilon^2-1)}{2\sqrt{z(z+\varepsilon^2)(1+\varepsilon^2z)}} & -\frac{\varepsilon^2(z+1)}{2\sqrt{z(z+\varepsilon^2)(1+\varepsilon^2z)}} \\ -\frac{z(z+1)}{2\sqrt{z(z+\varepsilon^2)(1+\varepsilon^2z)}} & \frac{1}{2} + \frac{z(\varepsilon^2-1)}{2\sqrt{z(z+\varepsilon^2)(1+\varepsilon^2z)}} \end{pmatrix}\end{aligned}$$

and

$$(13) \quad \begin{aligned}F_{\varepsilon,2}(z) &= E_\varepsilon(z) \begin{pmatrix} 0 & 0 \\ 0 & 1 \end{pmatrix} E_\varepsilon(z)^{-1} \\ &= \begin{pmatrix} \frac{1}{2} + \frac{z(\varepsilon^2-1)}{2\sqrt{z(z+\varepsilon^2)(1+\varepsilon^2z)}} & \frac{\varepsilon^2(z+1)}{2\sqrt{z(z+\varepsilon^2)(1+\varepsilon^2z)}} \\ \frac{z(z+1)}{2\sqrt{z(z+\varepsilon^2)(1+\varepsilon^2z)}} & \frac{1}{2} - \frac{z(\varepsilon^2-1)}{2\sqrt{z(z+\varepsilon^2)(1+\varepsilon^2z)}} \end{pmatrix}\end{aligned}$$

Lastly we define the function,

$$(14) \quad g_{\alpha,\beta}(z) = \frac{2z(1 + \alpha^2\beta^2) + \beta^2(z^2 + 1) + \alpha^2(z^2 + 1)}{4\sqrt{(z + \alpha^2)(1 + \alpha^2z)(z + \beta^2)(1 + \beta^2z)}}$$

Note that  $g_{\alpha,\beta}(z) = g_{\beta,\alpha}(z)$ . We are now prepared to state the main theorem of this paper,

**Theorem 2.1.** *Let  $-N \leq \xi, \xi' \leq -1$  and  $0 < m < N$ . The split two-periodic Aztec diamond of size  $2N$  has correlation kernel given by*

$$(15) \quad \left[ \mathbb{K}_N(4m', 2\xi' + j; 4m, 2\xi + i) \right]_{i,j=0}^1 = -\frac{\mathbb{I}_{m > m'}}{2\pi i} \oint_{\gamma_{0,1}} \frac{dz}{z} z^{\xi' - \xi} \Phi_\alpha(z)^{\frac{N}{2} - m'} \Phi_\varepsilon(z)^{m - \frac{N}{2}} \\ + \frac{1}{(2\pi i)^2} \oint_{\gamma_1} dw \oint_{\gamma_{0,1}} \frac{dz}{z(z-w)} \frac{w^{\xi' + N} (z-1)^N}{z^{\xi + N} (w-1)^N} r_{\alpha,1}(w)^{\frac{N}{2} - m'} F_{\alpha,1}(w) \Phi_\varepsilon(z)^{m - \frac{N}{2}} \\ + \frac{1}{(2\pi i)^2} \oint_{\gamma_1} dw \oint_{\gamma_{0,1}} \frac{dz}{z(z-w)} \frac{w^{\xi' + N} (z-1)^N}{z^{\xi + N} (w-1)^N} r_{\alpha,2}(w)^{\frac{N}{2} - m'} \frac{2F_{\alpha,2}(w) F_{\beta,1}(w) F_{\alpha,1}(w)}{1 + 2g_{\alpha,\beta}(w)} \Phi_\varepsilon(z)^{m - \frac{N}{2}}$$

when  $0 < m' \leq N/2$  and

$$(16) \quad \left[ \mathbb{K}_N(4m', 2\xi' + j; 4m, 2\xi + i) \right]_{i,j=0}^1 = -\frac{\mathbb{I}_{m < m'}}{2\pi i} \oint_{\gamma_{0,1}} \frac{dz}{z} z^{\xi - \xi'} \Phi_\beta(z)^{\frac{N}{2} - m'} \Phi_\varepsilon(z)^{m - \frac{N}{2}} \\ + \frac{1}{(2\pi i)^2} \oint_{\gamma_1} dw \oint_{\gamma_{0,1}} \frac{dz}{z(z-w)} \frac{w^{\xi' + N} (z-1)^N}{z^{\xi + N} (w-1)^N} r_{\beta,1}(w)^{\frac{N}{2} - m'} \frac{2}{1 + 2g_{\alpha,\beta}(w)} F_{\beta,1}(w) F_{\alpha,1}(w) \Phi_\varepsilon(z)^{m - \frac{N}{2}}$$

when  $N/2 < m' < N$ . Here  $\gamma_1$  is a contour surrounding 1 and  $\gamma_{0,1}$  is a contour surrounding 0 and  $\gamma_1$ . Both contours are oriented in the positive direction. In both cases if  $m \leq N/2$  then  $\varepsilon = \alpha$  and if  $m > N/2$  then  $\varepsilon = \beta$ .

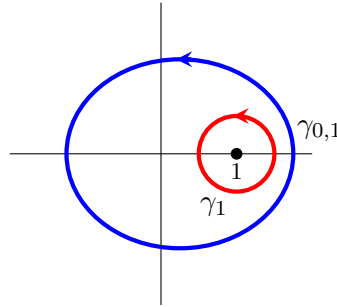


FIGURE 6. Depiction of the contours  $\gamma_{0,1}$  and  $\gamma_1$ .

Figure 6 depicts the contours from the above formula. The proof of Theorem 2.1 is in Section 3, with some details deferred to Sections 5 and 6.

The kernel presented in Theorem 2.1 has somewhat different forms depending on which side of the interface the vertex  $(4m', 2\xi' + j)$  is on, however this is simply due to the way the kernel is derived. The following corollary illustrates that there is a symmetry to the correlation kernel when we flip the model about the interface.



**Corollary 2.1.** For  $N/2 < m' < N$  the correlation kernel of the split two periodic Aztec diamond may be written as,

$$(17) \quad \left[ \mathbb{K}_N(4m', 2\xi' + j; 4m, 2\xi + i) \right]_{i,j=0}^1 = -\frac{\mathbb{I}_{m>m'}}{2\pi i} \oint_{\gamma_{0,1}} \frac{dz}{z} z^{\xi'-\xi} \Phi_\beta(z)^{\frac{N}{2}-m'} \Phi_\varepsilon(z)^{m-\frac{N}{2}} \\ + \frac{1}{(2\pi i)^2} \oint_{\gamma_1} dw \oint_{\gamma_{0,1}} \frac{dz}{z(z-w)} \frac{w^{\xi'+N}(z-1)^N}{z^{\xi+N}(w-1)^N} r_{\beta,1}(w)^{\frac{N}{2}-m'} F_{\beta,1}(w) \Phi_\varepsilon(z)^{m-\frac{N}{2}} \\ + \frac{1}{(2\pi i)^2} \oint_{\gamma_1} dw \oint_{\gamma_{0,1}} \frac{dz}{z(z-w)} \frac{w^{\xi'+N}(z-1)^N}{z^{\xi+N}(w-1)^N} r_{\beta,2}(w)^{\frac{N}{2}-m'} \frac{2}{1+2g_{\alpha,\beta}(w)} F_{\beta,2}(w) F_{\alpha,1}(w) F_{\beta,1}(w) \Phi_\varepsilon(z)^{m-\frac{N}{2}}$$

This corollary is proven at the end of Section 3. Despite the fact that the initial form of the kernel was more compact, this expression of the kernel is more useful for making comparisons to the typical two-periodic model, which we consider below in Section 2.2. The statement in Corollary 2.1 also allows us to state the kernel succinctly for any  $0 < m' < N$ ,

$$(18) \quad \left[ \mathbb{K}_N(4m', 2\xi' + j; 4m, 2\xi + i) \right]_{i,j=0}^1 = -\frac{\mathbb{I}_{m>m'}}{2\pi i} \oint_{\gamma_{0,1}} \frac{dz}{z} z^{\xi'-\xi} \Phi_{\varepsilon(m')}(z)^{\frac{N}{2}-m'} \Phi_{\varepsilon(m)}(z)^{m-\frac{N}{2}} \\ + \frac{1}{(2\pi i)^2} \sum_{k=1,2} \oint_{\gamma_1} dw \oint_{\gamma_{0,1}} \frac{dz}{z(z-w)} \frac{w^{\xi'+N}(z-1)^N}{z^{\xi+N}(w-1)^N} r_{\varepsilon(m'),1}(w)^{\frac{N}{2}-m'} r_{\varepsilon(m),k}(z)^{m-\frac{N}{2}} F_{\varepsilon(m'),1}(w) F_{\varepsilon(m),k}(z) \\ + \frac{1}{(2\pi i)^2} \sum_{k=1,2} \oint_{\gamma_1} dw \oint_{\gamma_{0,1}} \frac{dz}{z(z-w)} \frac{w^{\xi'+N}(z-1)^N}{z^{\xi+N}(w-1)^N} r_{\varepsilon(m'),2}(w)^{\frac{N}{2}-m'} r_{\varepsilon(m),k}(z)^{m-\frac{N}{2}} \\ \times \frac{2}{1+2g_{\alpha,\beta}(w)} F_{\varepsilon(m'),2}(w) F_{\bar{\varepsilon}(m'),1}(w) F_{\varepsilon(m'),1}(w) F_{\varepsilon(m),k}(z)$$

Here we use the following notation,

$$(\varepsilon(m), \bar{\varepsilon}(m)) = \begin{cases} (\alpha, \beta) & \text{if } m \leq N/2 \\ (\beta, \alpha) & \text{if } m > N/2 \end{cases}$$

In instances where we know that both vertices are on the same side of the interface, we use the shorthand notation,

$$(\varepsilon, \bar{\varepsilon}) = \begin{cases} (\alpha, \beta) & \text{if } m', m \leq N/2 \\ (\beta, \alpha) & \text{if } m', m > N/2 \end{cases}$$

In equation (18) we have also taken the additional step and expanded the matrix  $\phi_\varepsilon(z)$  in terms of its eigen-decomposition.

**2.2. Comparison to the Two-Periodic Aztec Diamond.** Before we analyze the behavior of the model, we first want to comment on the form of the correlation kernel in (18) and how it relates to the correlation kernel of the typical two-periodic Aztec diamond. We recover the typical two-periodic Aztec diamond from the split two-periodic Aztec diamond by setting  $\alpha = \beta = \varepsilon$ . The correlation kernel of the two-periodic Aztec diamond, as formulated in [3], can be stated using the notation presented in this paper as

**Theorem** ([3], Theorem 5.2). *Let  $-N \leq \xi, \xi' \leq -1$  and  $0 < m < N$ . The two-periodic Aztec diamond of size  $2N$  has correlation kernel given by*

$$(19) \quad \left[ \mathbb{K}_{TP,N}^\varepsilon(4m', 2\xi' + j; 4m, 2\xi + i) \right]_{i,j=0}^1 = -\frac{\mathbb{I}_{m>m'}}{2\pi i} \oint_{\gamma_{0,1}} \frac{dz}{z} z^{\xi'-\xi} \Phi_\varepsilon(z)^{m-m'}$$

$$+ \frac{1}{(2\pi i)^2} \sum_{k=1,2} \oint_{\gamma_1} dw \oint_{\gamma_{0,1}} \frac{dz}{z(z-w)} \frac{w^{\xi'+N}(z-1)^N}{z^{\xi+N}(w-1)^N} r_{\varepsilon,1}(w)^{\frac{N}{2}-m'} r_{\varepsilon,k}(z)^{m-\frac{N}{2}} F_{\varepsilon,1}(w) F_{\varepsilon,k}(z)$$

Now consider the split two-periodic Aztec diamond under the condition that the coordinates lie on the same side of the interface, e.g.  $m, m' \leq N/2$  or  $m, m' \geq N/2$ . The correlation kernel under these conditions simplifies to,

$$(20) \quad \left[ \mathbb{K}_N(4m', 2\xi' + j; 4m, 2\xi + i) \right]_{i,j=0}^1 = \left[ \mathbb{K}_{TP,N}^\varepsilon(4m', 2\xi' + j; 4m, 2\xi + i) \right]_{i,j=0}^1$$

$$+ \frac{1}{(2\pi i)^2} \sum_{k=1,2} \oint_{\gamma_1} dw \oint_{\gamma_{0,1}} \frac{dz}{z(z-w)} \frac{w^{\xi'+N}(z-1)^N}{z^{\xi+N}(w-1)^N} r_{\varepsilon,2}(w)^{\frac{N}{2}-m'} r_{\varepsilon,k}(z)^{m-\frac{N}{2}}$$

$$\times \frac{2}{1 + 2g_{\alpha,\beta}(w)} F_{\varepsilon,2}(w) F_{\varepsilon,1}(w) F_{\varepsilon,1}(w) F_{\varepsilon,k}(z)$$

From this expression we see how the correlation kernel of the split model relates to the typically two-periodic model. In order to understand how the local asymptotics of the split two-periodic Aztec diamond differ from the local asymptotics of the typical two-periodic Aztec diamond we only need to understand the asymptotics of the additional two double contour integrals. These will be our main focus when describing the local asymptotics in Section 2.4.

**2.3. Classification of the Macroscopic Regions.** Before we compute the explicit local asymptotics of the model, we would like to introduce the saddle functions associated with the kernel of the model. In doing so, we will consider the behavior of the model around some *asymptotic coordinate*. Let  $(x, y) \in (0, 1/2) \cup (1/2, 1) \times (-1, 0)$ , where we omit the case where the asymptotic coordinate is exactly on the interface of the model. By letting  $(m, \xi) = (xN, yN)$ , the vertex  $(4m, 2\xi + i)$  has asymptotic coordinate  $(x, y)$ . Now we define the functions,

$$(21) \quad \psi_{\varepsilon,k}(z; x, y) = (y + 1) \log z - \log(z - 1) + \left( \frac{1}{2} - x \right) \log r_{\varepsilon,k}(z)$$

where  $k = 1, 2$ . These functions play a crucial role in the asymptotics of the typical two-periodic Aztec diamond and are also key to understanding the asymptotics of the split two-periodic model.

**Remark 2.1.** *The saddle functions  $\psi_{\varepsilon,k}(z)$  are, up to a scalar and change of parameters, the saddle functions defined and analyzed in [11].*

In other words, most of the analytic work we need in order to prepare our integrals for saddle point methods was accomplished in [11]. We state the saddle functions in [11, p. 15] for comparison.

$$\Phi_k(z) = -(1 + \xi_2) \log z + 2 \log(z - 1) + \xi_1 \log \lambda_k(z)$$

where  $k = 1, 2$ . They define

$$\lambda_{1,2}(z) = \frac{\left( (\alpha + \beta)z \pm \sqrt{z(z + \alpha^2)(z + \beta^2)} \right)^2}{z(z - 1)^2}$$

and  $-1 < \xi_1, \xi_2 < 1$  are parameters that define the asymptotic coordinate, albeit different from our  $x$  and  $y$ . Note that the above  $\alpha$  and  $\beta$  are from the convention in [11] and not the same  $\alpha$  and  $\beta$

presented in this text. Letting  $\alpha = \varepsilon$  and  $\beta = \varepsilon^{-1}$  it is easy to check that,

$$r_{\varepsilon,k}(z) = \lambda_k(z)$$

for  $k = 1, 2$ . Using the change of parameter,  $\xi_1 = 2x - 1$  and  $\xi_2 = 2y + 1$ , we obtain

$$\Phi_k(z) = -2\psi_{\varepsilon,k}(z; x, y)$$

Much like the two-periodic Aztec diamond, the split two-periodic model contains all three possible regions: smooth, rough, and frozen. The following piece-wise saddle function will help us succinctly define the boundary between these macroscopic regions.

$$(22) \quad \psi_k(z) = \begin{cases} \psi_{\alpha,k}(z; x, y) & \text{for } x < 1/2 \\ \psi_{\beta,k}(z; x, y) & \text{for } x > 1/2 \end{cases}$$

For fixed  $(x, y)$  we can think of the saddle functions  $\psi_1(z)$  and  $\psi_2(z)$  as a single function,  $\Psi(z)$ , on some Riemann surface. The Riemann surface is two sheets of  $\mathbb{C}$  glued together along the branch cuts of  $\psi_k(z)$ .<sup>3</sup> On one sheet of the surface,  $\Psi(z) = \psi_1(z)$ , while on the other sheet,  $\Psi(z) = \psi_2(z)$ . Note that we can consider  $\Psi(z)$  to be a multivariate function on some Riemann surface as long as we restrict our asymptotic coordinate to one side of the interface.

As long as  $(x, y)$  is not on some boundary between regions, the function  $\Psi(z)$  has a total of four simple saddle points. The location of these saddle points on the Riemann surface classify the macroscopic region of the model.

**Definition 2.1.** *Let  $(x, y) \in (0, 1/2) \cup (1/2, 1) \times (-1, 0)$  denote the asymptotic coordinate on the Aztec diamond.*

- (1) *If there are two saddles points on either copy of the positive real axis, then  $(x, y) \in \mathfrak{F}$ , the frozen region of the model.*
- (2) *If there are two complex saddle points (on either sheet of the Riemann surface), then  $(x, y) \in \mathfrak{R}$ , the rough region of the model.*
- (3) *If all four saddle points are located on either copy of the negative real axis away from the branch cuts, then  $(x, y) \in \mathfrak{S}$ , the smooth region of the model.*

This is the same definition of regions presented for the typical two-periodic model in [11, Definition 2.9]. The saddle function,  $\Psi(z)$ , can also be used to determine the boundaries between the macroscopic regions. Any point where saddle points coalesce and there is a double or triple saddle point is on some boundary between the macroscopic regions. Additionally, due to the piece wise nature of the saddle functions, we must check for transitions along the line  $x = 1/2$ . Figure 7 depicts an example of the macroscopic boundaries for a split two-periodic model.

For either half of the model, the definition and boundaries between macroscopic regions agree with the typically two-periodic case.<sup>4</sup> In the section below we will show how this follows from the local asymptotics of the correlation kernel.

**2.4. Asymptotic Behavior.** In this work, we will focus our asymptotic results to the local behavior of the model away from the interface. We define the coordinates in the following manner,

$$(23) \quad m = xN + x_1 \qquad m' = xN + x_2$$

$$(24) \quad \xi = yN + y_1 \qquad \xi' = yN + y_2$$

<sup>3</sup>The branch cuts are dependent on  $x$ . If  $x < 1/2$ , then the branch cuts are  $(-\infty, -\alpha^{-2}] \cup [-\alpha^2, 0]$ , while if  $x > 1/2$  the branch cuts are  $(-\infty, -\beta^{-2}] \cup [-\beta^2, 0]$ .

<sup>4</sup>See [11] for a similar classification in the two periodic case.

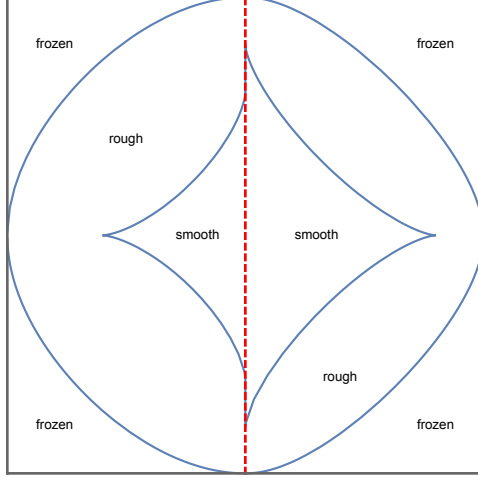


FIGURE 7. Boundaries between macroscopic regions of the split Aztec diamond when  $\alpha = 1/2$  and  $\beta = 1/3$ . The dashed red line denoted the interface of the model. Boundary computed numerically using Mathematica.

where we assume  $x \neq 1/2$ , and  $x_1$  and  $x_2$  are small enough in magnitude so that the coordinates  $(4m, 2\xi + i)$  and  $(4m', 2\xi' + j)$  lie on the same side of the interface. Under these considerations, we rewrite correlation kernel in terms of the saddle functions,

$$(25) \quad \left[ \mathbb{K}_N(4m', 2\xi' + j; 4m, 2\xi + i) \right]_{i,j=0}^1 = \left[ \mathbb{K}_{TP,N}^\varepsilon(4m', 2\xi' + j; 4m, 2\xi + i) \right]_{i,j=0}^1 \\ + \frac{1}{(2\pi i)^2} \sum_{k=1,2} \oint_{\gamma_1} dw \oint_{\gamma_{0,1}} dz \frac{2}{z(z-w)1+2g_{\alpha,\beta}(w)} F_{\varepsilon,2}(w) F_{\bar{\varepsilon},1}(w) F_{\varepsilon,1}(w) F_{\varepsilon,k}(z) \\ \times \exp [N(\psi_2(w; x, y) - \psi_k(z; x, y)) + \varphi_{\varepsilon,2}(w; x_2, y_2) - \varphi_{\varepsilon,k}(z; x_1, y_1)]$$

The saddle function  $\psi_k(z)$  is defined in equation (22) and we define the function  $\varphi_{\varepsilon,k}(z; x_1, y_1)$  as

$$(26) \quad \varphi_{\varepsilon,k}(z; x_1, y_1) = y_1 \log z - x_1 \log r_{\varepsilon,k}(z)$$

For brevity we will let

$$(27) \quad \left[ I_{2,k}^\varepsilon(4m', 2\xi' + j; 4m, 2\xi + i) \right]_{i,j=0}^1 = \frac{1}{(2\pi i)^2} \oint_{\gamma_1} dw \oint_{\gamma_{0,1}} dz \frac{2}{z(z-w)1+2g_{\alpha,\beta}(w)} F_{\varepsilon,2}(w) F_{\bar{\varepsilon},1}(w) F_{\varepsilon,1}(w) \\ \times F_{\varepsilon,k}(z) \exp [N(\psi_2(w; x, y) - \psi_k(z; x, y)) + \varphi_{\varepsilon,2}(w; x_2, y_2) - \varphi_{\varepsilon,k}(z; x_1, y_1)]$$

for  $k = 1, 2$ . So we may write the kernel, briefly, as

$$(28) \quad \left[ \mathbb{K}_N(4m', 2\xi' + j; 4m, 2\xi + i) \right]_{i,j=0}^1 = \left[ \mathbb{K}_{TP,N}^\varepsilon(4m', 2\xi' + j; 4m, 2\xi + i) \right]_{i,j=0}^1 \\ + \sum_{k=1,2} \left[ I_{2,k}^\varepsilon(4m', 2\xi' + j; 4m, 2\xi + i) \right]_{i,j=0}^1$$

Thus the local asymptotics of the split model depends on the asymptotics of the typically two-periodic Aztec diamond along with the asymptotics of the contour integrals  $I_{2,1}^\varepsilon$  and  $I_{2,2}^\varepsilon$ . The local asymptotics of the two-periodic Aztec diamond are well studied, so we will focus on the asymptotic behavior of these two additional contour integrals.

We will utilize the symmetry of the kernel and just consider the asymptotics on the  $\alpha$ -side of the interface, e.g. when  $x < 1/2$ . In doing so, we should consider two cases:

- (a)  $0 < \beta < \alpha < 1$
- (b)  $0 < \alpha < \beta < 1$

The behavior of the double contour integrals  $I_{2,2}^\alpha$  does not depend on the macroscopic region of the model, however, if we are in case (b), the decay of  $I_{2,2}^\alpha$  does depend on the region of the model in other ways. Consider the regions of the model where  $(x, y)$  satisfies one of the following inequalities:

- (i)  $\psi'_{\alpha,2}(-\beta^2; x, y) > 0$
- (ii)  $\psi'_{\alpha,2}(-\beta^{-2}; x, y) < 0$

Since  $\psi'_{\alpha,2}(z)$  is linear in  $x$  and  $y$ , the inequalities just denote trapezoidal regions of the model. Note that these regions are empty if  $\beta < \alpha$ . The exact size and shape of these regions depends on the exact values of  $\alpha$  and  $\beta$ . Figure 8 gives examples of these regions for different values of  $\alpha$  and  $\beta$ .

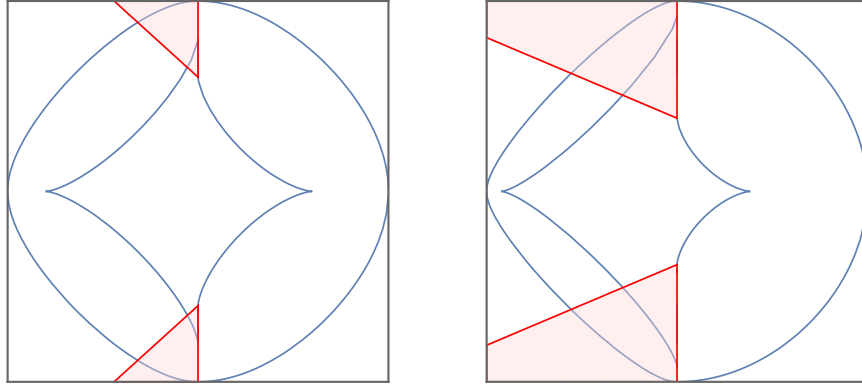


FIGURE 8. Regions where  $I_{2,2}^\alpha(4m', 2\xi' + j; 4m, 2\xi + i)$  decays non-exponentially are shaded in red. On the left side figure,  $\beta = 1/2$  and  $\alpha = 1/3$ , while on the right side figure,  $\beta = 2/3$  and  $\alpha = 1/5$ .

We will denote the asymptotic region where either (i) or (ii) is satisfied as the *strong-coupling* region of the model, denoted  $\mathfrak{C}$ . We state the following asymptotic results regarding the behavior of  $I_{2,2}^\alpha(4m', 2\xi' + j; 4m, 2\xi + i)$ ,

**Proposition 2.1.** *Let  $(m, \xi)$  and  $(m', \xi')$  be given by equations (23) and (24) such that  $x < 1/2$ , then*

$$|I_{2,2}^\alpha(4m', 2\xi' + j; 4m, 2\xi + i)| \leq c_2 e^{-c_1 N} \quad \text{or} \quad |I_{2,2}^\alpha(4m', 2\xi' + j; 4m, 2\xi + i)| \leq c_3 N^{-1}$$

where  $c_1$ ,  $c_2$ , and  $c_3$  are positive constants. The latter occurring when only when  $(x, y) \in \mathfrak{C}$ .

The behavior of the second double contour integral,  $I_{2,1}^\alpha(4m', 2\xi' + j; 4m, 2\xi + i)$ , depends on the macroscopic region of the model and also on the strong-coupling region described above. We focus our attention on the behavior of this integral in the rough and smooth regions of the model only. We state the following results,

**Proposition 2.2.** *Let  $(m, \xi)$  and  $(m', \xi')$  be given by equations (23) and (24) such that  $x < 1/2$ .*

- (1) *If  $(x, y) \in \mathfrak{R}$ , then*

$$|I_{2,1}^\alpha(4m', 2\xi' + j; 4m, 2\xi + i)| \leq c N^{-1}$$

for some positive constant  $c$ .

(2) If  $(x, y) \in \mathfrak{S}$  and  $(x, y) \notin \mathfrak{C}$ , then

$$|I_{2,1}^\alpha(4m', 2\xi' + j; 4m, 2\xi + i)| \leq ce^{-c_1 N}$$

for some positive constants  $c$  and  $c_1$ .

(3) If  $(x, y) \in \mathfrak{S}$  and  $(x, y) \in \mathfrak{C}$ , then

$$|I_{2,1}^\alpha(4m', 2\xi' + j; 4m, 2\xi + i)| \leq cN^{-1}$$

for some positive constant  $c$ .

Lastly, we should mention how these results combine with the local asymptotic behavior of the typical two-periodic kernel. The local asymptotics for the two-periodic Aztec diamond were initially stated in [7, Theorem 2.6]. Let  $\mathbb{K}_{FP}^\varepsilon(\bar{p}_1; \bar{p}_2)$  denote the full plane correlation kernel for the infinite square lattice with the same two-periodic weighting as the two-periodic Aztec diamond described in Section 2.2. The results from [7, Theorem 2.6] and also [11, Theorem 2.10] state<sup>5</sup> that if  $(x, y) \in \mathfrak{S}$  then,

$$(29) \quad \mathbb{K}_{TP,N}^\varepsilon(4m', 2\xi' + j; 4m, 2\xi + i) = \mathbb{K}_{FP}^\varepsilon(x_1, y_1; x_2, y_2) + O(e^{-cN})$$

However, in the case of the split two-periodic Asymptotic we see a difference in the sub leading order term. In particular, we wish to highlight that if  $(x, y) \in \mathfrak{S} \cap \mathfrak{C}$  then

$$(30) \quad \mathbb{K}_{TP,N}^\varepsilon(4m', 2\xi' + j; 4m, 2\xi + i) = \mathbb{K}_{FP}^\varepsilon(x_1, y_1; x_2, y_2) + O(N^{-1})$$

In the region  $\mathfrak{S} \cap \mathfrak{C}$ , not only do the additional integrals contribute to the sub-leading order term, but they change the decay of it significantly.

### 3. DERIVATION OF THE CORRELATION KERNEL

Our main goal in this section is to prove the results stated in Theorem 2.1. In order to prove Theorem 2.1, we start in Section 3.1 by stating an intermediate version of the kernel which can be derived by using techniques from [3]. The form of the kernel differs slightly depending on whether the coordinate  $(4m', 2\xi' + j)$  is on the  $\alpha$ -side or  $\beta$ -side of the interface. In Section 3.2, we prove the statement of the kernel for  $m' \leq N/2$  and in Section 3.3, we prove the statement of the kernel for  $m' > N/2$ . After deriving the kernel, we prove the statement given in Corollary 2.1, which illustrates the symmetry of the kernel and the relationship of the kernel to the typical two-periodic Aztec diamond. This work is done in Section 3.4.

**3.1. An Intermediate Correlation Kernel.** We start by introducing some more necessary notation. We define,

$$(31) \quad \phi_N(z) = \Phi_\alpha(z)^{\frac{N}{2}} \Phi_\beta(z)^{\frac{N}{2}}$$

and its eigen-decomposition,

$$(32) \quad \phi_N(z) = r_{1,N}(z)F_{1,N}(z) + r_{2,N}(z)F_{2,N}(z)$$

The explicit formulas for the eigenvalues and matrices are quite involved. We can, however, write the trace of  $\phi_N(z)$  in a rather succinct way. We let,

$$(33) \quad t_N(z) = \text{tr } \phi_N(z) = \left( \frac{1}{2} + g_{\alpha,\beta}(z) \right) \left( r_{\alpha,1}(z)^{\frac{N}{2}} r_{\beta,1}(z)^{\frac{N}{2}} + r_{\alpha,2}(z)^{\frac{N}{2}} r_{\beta,2}(z)^{\frac{N}{2}} \right) \\ + \left( \frac{1}{2} - g_{\alpha,\beta}(z) \right) \left( r_{\alpha,2}(z)^{\frac{N}{2}} r_{\beta,1}(z)^{\frac{N}{2}} + r_{\alpha,1}(z)^{\frac{N}{2}} r_{\beta,2}(z)^{\frac{N}{2}} \right)$$

---

<sup>5</sup>The original results in [7] just focus along a diagonal of the model, the later results [11] look at the entire smooth region.

where the function  $g_{\alpha,\beta}(z)$  is defined in equation (14). Since  $\det \phi_N(z) = 1$ , the eigenvalues of  $\phi_N(z)$  can be expressed as,

$$(34) \quad r_{1,N}(z) = \frac{1}{2} \left( t_N(z) + \sqrt{t_N(z)^2 - 4} \right) \quad r_{2,N}(z) = \frac{1}{2} \left( t_N(z) - \sqrt{t_N(z)^2 - 4} \right)$$

If  $E_N(z)$  is the eigenvector matrix that respects this ordering of eigenvalues, then  $F_{k,N}(z)$  are the matrices,

$$(35) \quad F_{1,N}(z) = E_N(z) \begin{pmatrix} 1 & 0 \\ 0 & 0 \end{pmatrix} E_N(z)^{-1} \quad F_{2,N}(z) = E_N(z) \begin{pmatrix} 0 & 0 \\ 0 & 1 \end{pmatrix} E_N(z)^{-1}$$

We now may state,

**Lemma 3.1.** *Let  $0 < m < N$ , and  $-N \leq \xi, \xi' \leq -1$ . The split two-periodic Aztec diamond of size  $2N$  has a correlation kernel given by,*

$$(36) \quad \left[ \mathbb{K}_N(4m', 2\xi' + j; 4m, 2\xi + i) \right]_{i,j=0}^1 = -\frac{\mathbb{I}_{m>m'}}{2\pi i} \oint_{\gamma_{0,1}} \frac{dz}{z} z^{\xi'-\xi} \Phi_\alpha(z)^{\frac{N}{2}-m'} \Phi_\varepsilon(z)^{m-\frac{N}{2}} \\ + \frac{1}{(2\pi i)^2} \oint_{\gamma_1} dw \oint_{\gamma_{0,1}} \frac{dz}{z(z-w)} \frac{w^{\xi'+N}(z-1)^N}{z^{\xi+N}(w-1)^N} \Phi_\alpha(w)^{-m'} F_{1,N}(w) \Phi_\alpha(w)^{\frac{N}{2}} \Phi_\varepsilon(z)^{m-\frac{N}{2}}$$

when  $0 < m' \leq N/2$ . Alternatively, when  $N/2 < m' < N$ , the correlation kernel is

$$(37) \quad \left[ \mathbb{K}_N(4m', 2\xi' + j; 4m, 2\xi + i) \right]_{i,j=0}^1 = -\frac{\mathbb{I}_{m>m'}}{2\pi i} \oint_{\gamma_{0,1}} \frac{dz}{z} z^{\xi'-\xi} \Phi_\alpha(z)^{\frac{N}{2}-m'} \Phi_\varepsilon(z)^{m-\frac{N}{2}} \\ + \frac{1}{(2\pi i)^2} \oint_{\gamma_1} dw \oint_{\gamma_{0,1}} \frac{dz}{z(z-w)} \frac{w^{\xi'+N}(z-1)^N}{z^{\xi+N}(w-1)^N} \Phi_\beta(w)^{\frac{N}{2}-m'} \Phi_\alpha(w)^{-\frac{N}{2}} F_{1,N}(w) \Phi_\alpha(w)^{\frac{N}{2}} \Phi_\varepsilon(z)^{m-\frac{N}{2}}$$

The contours  $\gamma_1$  and  $\gamma_{0,1}$  are the same contours detailed in Theorem 2.1.

The proof of the above lemma is deferred to Section 5. While we now have a correlation kernel for the process, this kernel is not set up well for asymptotic analysis. The main part of the proof of Theorem 2.1 manipulates the above kernel in a way that simplifies the analysis.

**3.2. Proof of Theorem 2.1 when  $0 < m' \leq N/2$ .** First recall that we can decompose the matrix  $\Phi_\alpha(w)$  in the following manner,

$$\Phi_\alpha(w) = r_{\alpha,1}(w)F_{\alpha,1}(w) + r_{\alpha,2}(w)F_{\alpha,2}(w)$$

where  $r_{\alpha,k}(w)$  and  $F_{\alpha,k}(w)$  are given by equations (10)-(13). Plugging this formula into the double contour integral from Lemma 3.1 gives,

$$(38) \quad \left[ \mathbb{K}_N(4m', 2\xi' + j; 4m, 2\xi + i) \right]_{i,j=0}^1 = -\frac{\mathbb{I}_{m>m'}}{2\pi i} \oint_{\gamma_{0,1}} \frac{dz}{z} z^{\xi'-\xi} \Phi_\alpha(z)^{\frac{N}{2}-m'} \Phi_\varepsilon(z)^{m-\frac{N}{2}} \\ + \frac{1}{(2\pi i)^2} \sum_{k_1=1,2} \sum_{k_2=1,2} \oint_{\gamma_1} dw \oint_{\gamma_{0,1}} \frac{dz}{z(z-w)} \frac{w^{\xi'+N}(z-1)^N}{z^{\xi+N}(w-1)^N} r_{\alpha,k_1}(w)^{-m'} r_{\alpha,k_2}(w)^{\frac{N}{2}} \\ \times F_{\alpha,k_1}(w)F_{1,N}(w)F_{\alpha,k_2}(w)\Phi_\varepsilon(z)^{m-\frac{N}{2}}$$

Our goal is to replace the matrix product  $F_{\alpha,k_1}(w)F_{1,N}(w)$ , as the matrix  $F_{1,N}(w)$  is hard to state precisely and thus is not amenable to asymptotic analysis. We start by rearranging equation (32),

$$(39) \quad F_{1,N}(w) = r_{1,N}(w)^{-1}\phi_N(w) - r_{1,N}(w)^{-1}r_{2,N}(w)F_{2,N}(w) \\ = r_{2,N}(w)\phi_N(w) - r_{2,N}(w)^2F_{2,N}(w)$$

Above we have utilized the fact that  $r_{1,N}(w) = r_{2,N}(w)^{-1}$ . Now we plug the eigen-decompositions of  $\Phi_\alpha(w)$  and  $\Phi_\beta(w)$  into equation (31) to obtain,

$$\phi_N(w) = \left( r_{\alpha,1}(w)^{\frac{N}{2}} F_{\alpha,1}(w) + r_{\alpha,2}(w)^{\frac{N}{2}} F_{\alpha,2}(w) \right) \left( r_{\beta,1}(w)^{\frac{N}{2}} F_{\beta,1}(w) + r_{\beta,2}(w)^{\frac{N}{2}} F_{\beta,2}(w) \right)$$

This means that

$$(40) \quad F_{\alpha,k_1}(w)\phi_N(w) = r_{\alpha,k_1}(w)^{\frac{N}{2}} F_{\alpha,k_1}(w) \left( r_{\beta,1}(w)^{\frac{N}{2}} F_{\beta,1}(w) + r_{\beta,2}(w)^{\frac{N}{2}} F_{\beta,2}(w) \right)$$

Combining the above with equation (39) gives,

$$(41) \quad F_{\alpha,1}(w)F_{1,N}(w) = r_{2,N}(w)r_{\alpha,1}(w)^{\frac{N}{2}}r_{\beta,1}(w)^{\frac{N}{2}}F_{\alpha,1}(w)F_{\beta,1}(w) \\ + r_{2,N}(w)r_{\alpha,1}(w)^{\frac{N}{2}}r_{\beta,2}(w)^{\frac{N}{2}}F_{\alpha,1}(w)F_{\beta,2}(w) - r_{2,N}(w)^2F_{\alpha,1}(w)F_{2,N}(w)$$

and

$$(42) \quad F_{\alpha,2}(w)F_{1,N}(w) = r_{2,N}(w)r_{\alpha,2}(w)^{\frac{N}{2}}r_{\beta,1}(w)^{\frac{N}{2}}F_{\alpha,2}(w)F_{\beta,1}(w) \\ + r_{2,N}(w)r_{\alpha,2}(w)^{\frac{N}{2}}r_{\beta,2}(w)^{\frac{N}{2}}F_{\alpha,2}(w)F_{\beta,2}(w) - r_{2,N}(w)^2F_{\alpha,2}(w)F_{2,N}(w)$$

We can now insert these replacements into the double contour integrals of the correlation kernel. There are a total of four double contour integrals in equation (38), each having the form,

$$\oint_{\gamma_1} \oint_{\gamma_{0,1}} \frac{dw dz}{z(z-w)} \frac{w^{\xi+N}(z-1)^N}{z^{\xi+N}(w-1)^N} r_{\alpha,k_1}(w)^{-m'} r_{\alpha,k_2}(w)^{\frac{N}{2}} F_{\alpha,k_1}(w) F_{1,N}(w) F_{\alpha,k_2}(w) F_{\varepsilon,k}(z) \Phi_\varepsilon(z)^{m-\frac{N}{2}}$$

To prevent our text from getting long, let's focus on only the following product

$$(43) \quad \frac{1}{(w-1)^N} r_{\alpha,k_1}(w)^{-m'} r_{\alpha,k_2}(w)^{\frac{N}{2}} F_{\alpha,k_1}(w) F_{1,N}(w)$$

This product contains all the terms relevant to the singularity (or zero) at  $w = 1$ . We would like to keep track of the order of this singularity/zero, as it is the only potentially non-analytic point inside  $\gamma_1$ . We will consider the expanded terms of this product when we substitute in equations (41) and (42). First, consider the product in (43) when  $k_1 = k_2 = 1$ ,

$$\frac{1}{(w-1)^N} r_{\alpha,k_1}(w)^{-m'} r_{\alpha,k_2}(w)^{\frac{N}{2}} F_{\alpha,k_1}(w) F_{1,N}(w) = \frac{r_{\alpha,1}(w)^{\frac{N}{2}-m'}}{(w-1)^N} F_{\alpha,1}(w) F_{1,N}(w)$$

Now using the replacement in (41) we get

$$(44) \quad \frac{r_{\alpha,1}(w)^{\frac{N}{2}-m'}}{(w-1)^N} F_{\alpha,1}(w) F_{1,N}(w) = \frac{r_{2,N}(w)r_{\alpha,1}(w)^{N-m'}r_{\beta,1}(w)^{\frac{N}{2}}}{(w-1)^N} F_{\alpha,1}(w) F_{\beta,1}(w) \\ + \frac{r_{2,N}(w)r_{\alpha,1}(w)^{N-m'}r_{\beta,2}(w)^{\frac{N}{2}}}{(w-1)^N} F_{\alpha,1}(w) F_{\beta,2}(w) - \frac{r_{2,N}(w)^2r_{\alpha,1}(w)^{\frac{N}{2}-m'}}{(w-1)^N} F_{\alpha,1}(w) F_{2,N}(w)$$

So we can consider each of these three terms, and their behavior at  $w = 1$ , separately. The scalar terms,

$$\frac{r_{2,N}(w)r_{\alpha,1}(w)^{N-m'}r_{\beta,2}(w)^{\frac{N}{2}}}{(w-1)^N}$$

and

$$\frac{r_{2,N}(w)^2r_{\alpha,1}(w)^{\frac{N}{2}-m'}}{(w-1)^N}$$

have no singularity at  $w = 1$ . To justify this statement we need the following two lemmas,

**Lemma 3.2.** *The following statements are true regarding the eigenvalues  $r_{\varepsilon,1}(z)$  and  $r_{\varepsilon,2}(z)$ :*



(1) For any  $\varepsilon \in (0, 1)$ ,  $r_{\varepsilon,1}(z)$  has a pole of order 2 at  $z = 1$  and  $r_{\varepsilon,2}(z)$  has a zero of order two at  $z = 1$ .

(2) For any  $\varepsilon \in (0, 1)$  and any  $z \in \mathbb{C} \setminus \{1\}$ ,  $r_{\varepsilon,1}(z)r_{\varepsilon,2}(z) = 1$ .

**Lemma 3.3.** *The eigenvalue  $r_{1,N}(z)$  has a pole of order  $2N$  at  $z = 1$  for all  $N$  and the eigenvalue  $r_{2,N}(z)$  has a zero of order  $2N$  at  $z = 1$  for all  $N$ .*

Lemma 3.2 follows from equations (10) and (11). Lemma 3.3 is a direct consequence of Lemma 3.6, which is stated later in this section and proven in Section 6. We also make note of two more lemmas,

**Lemma 3.4.** *For any  $\varepsilon \in (0, 1)$ , the matrix valued functions  $F_{\varepsilon,1}(z)$  and  $F_{\varepsilon,2}(z)$  are analytic for all  $z \in \mathbb{C} \setminus \{(-\infty, -\varepsilon^{-2}] \cup [-\varepsilon^2, 0]\}$ .*

**Lemma 3.5.** *The matrix-valued function  $F_{2,N}(z)$  has no pole at  $z = 1$ .*

Lemma 3.4 follows from equations (12) and (13). The proof of Lemma 3.5 is deferred to Section 6. By the residue theorem we can make the following simplification,

$$(45) \quad \oint_{\gamma_1} \oint_{\gamma_{0,1}} \frac{dw dz}{z(z-w)} \frac{w^{\xi'+N}(z-1)^N}{z^{\xi'+N}(w-1)^N} r_{\alpha,1}(w)^{\frac{N}{2}-m'} F_{\alpha,1}(w) F_{1,N}(w) F_{\alpha,1}(w) \Phi_\varepsilon(z)^{m-\frac{N}{2}}$$

$$= \oint_{\gamma_1} \oint_{\gamma_{0,1}} \frac{dw dz}{z(z-w)} \frac{w^{\xi'+N}(z-1)^N}{z^{\xi'+N}(w-1)^N} r_{2,N}(w) r_{\alpha,1}(w)^{N-m'} r_{\beta,1}(w)^{\frac{N}{2}}$$

$$\times F_{\alpha,1}(w) F_{\beta,1}(w) F_{\alpha,1}(w) \Phi_\varepsilon(z)^{m-\frac{N}{2}}$$

We now inspect equation (43) for all the other possible combinations of  $k_1$  and  $k_2$ . For each case, we replace the matrix product  $F_{\alpha,k_1}(w)F_{1,N}(w)$  with either equation (41) or (42). When  $k_1 = 1$  and  $k_2 = 2$  we obtain,

$$(46) \quad \frac{r_{\alpha,1}(w)^{-\frac{N}{2}-m'}}{(w-1)^N} F_{\alpha,1}(w) F_{1,N}(w) = \frac{r_{2,N}(w) r_{\alpha,1}(w)^{-m'} r_{\beta,1}(w)^{\frac{N}{2}}}{(w-1)^N} F_{\alpha,1}(w) F_{\beta,1}(w)$$

$$+ \frac{r_{2,N}(w) r_{\alpha,1}(w)^{-m'} r_{\beta,2}(w)^{\frac{N}{2}}}{(w-1)^N} F_{\alpha,1}(w) F_{\beta,2}(w) - \frac{r_{2,N}(w)^2 r_{\alpha,1}(w)^{-\frac{N}{2}-m'}}{(w-1)^N} F_{\alpha,1}(w) F_{2,N}(w)$$

All of the above terms have no pole at  $w = 1$ . Thus,

$$\oint_{\gamma_1} dw \oint_{\gamma_{0,1}} \frac{dz}{z(z-w)} \frac{w^{\xi'+N}(z-1)^N}{z^{\xi'+N}(w-1)^N} r_{\alpha,1}(w)^{-\frac{N}{2}-m'} F_{\alpha,1}(w) F_{1,N}(w) F_{\alpha,2}(w) \Phi_\varepsilon(z)^{m-\frac{N}{2}} = 0$$

For  $k_1 = 2$  and  $k_2 = 1$  the product in (43) is,

$$(47) \quad \frac{r_{\alpha,1}(w)^{\frac{N}{2}+m'}}{(w-1)^N} F_{\alpha,2}(w) F_{1,N}(w) = \frac{r_{2,N}(w) r_{\alpha,1}(w)^{m'} r_{\beta,1}(w)^{\frac{N}{2}}}{(w-1)^N} F_{\alpha,2}(w) F_{\beta,1}(w)$$

$$+ \frac{r_{2,N}(w) r_{\alpha,1}(w)^{m'} r_{\beta,2}(w)^{\frac{N}{2}}}{(w-1)^N} F_{\alpha,2}(w) F_{\beta,1}(w) - \frac{r_{2,N}(w)^2 r_{\alpha,1}(w)^{\frac{N}{2}+m'}}{(w-1)^N} F_{\alpha,2}(w) F_{2,N}(w)$$

In this case, the second and third terms have no pole at  $w = 1$ , so only the first term contribution non-trivially to the contour integral. Lastly we check equation (43) for the case  $k_1 = k_2 = 2$ ,

$$(48) \quad \frac{r_{\alpha,2}(w)^{\frac{N}{2}-m'}}{(w-1)^N} F_{\alpha,2}(w) F_{1,N}(w) = \frac{r_{2,N}(w) r_{\alpha,2}(w)^{N-m'} r_{\beta,2}(w)^{\frac{N}{2}}}{(w-1)^N} F_{\alpha,2}(w) F_{\beta,1}(w)$$

$$+ \frac{r_{2,N}(w) r_{\alpha,2}(w)^{N-m'} r_{\beta,2}(w)^{\frac{N}{2}}}{(w-1)^N} F_{\alpha,2}(w) F_{\beta,1}(w) - \frac{r_{2,N}(w)^2 r_{\alpha,2}(w)^{\frac{N}{2}-m'}}{(w-1)^N} F_{\alpha,2}(w) F_{2,N}(w)$$

All three terms have no singularity at  $w = 1$ , so the resulting double contour integral is trivial. This leaves us with the simplified kernel,

$$\begin{aligned}
(49) \quad & \left[ \mathbb{K}_N(4m', 2\xi' + j; 4m, 2\xi + i) \right]_{i,j=0}^1 = -\frac{\mathbb{I}_{m>m'}}{2\pi i} \oint_{\gamma_{0,1}} \frac{dz}{z} z^{\xi'-\xi} \Phi_\alpha(z)^{\frac{N}{2}-m'} \Phi_\varepsilon(z)^{m-\frac{N}{2}} \\
& + \frac{1}{(2\pi i)^2} \oint_{\gamma_1} dw \oint_{\gamma_{0,1}} \frac{dz}{z(z-w)} \frac{w^{\xi'+N}(z-1)^N}{z^{\xi+N}(w-1)^N} r_{2,N}(w) r_{\alpha,1}(w)^{N-m'} r_{\beta,1}(w)^{\frac{N}{2}} \\
& \quad \times F_{\alpha,1}(w) F_{\beta,1}(w) F_{\alpha,1}(w) \Phi_\varepsilon(z)^{m-\frac{N}{2}} \\
& + \frac{1}{(2\pi i)^2} \oint_{\gamma_1} dw \oint_{\gamma_{0,1}} \frac{dz}{z(z-w)} \frac{w^{\xi'+N}(z-1)^N}{z^{\xi+N}(w-1)^N} r_{2,N}(w) r_{\alpha,1}(w)^{m'} r_{\beta,1}(w)^{\frac{N}{2}} \\
& \quad \times F_{\alpha,2}(w) F_{\beta,1}(w) F_{\alpha,1}(w) \Phi_\varepsilon(z)^{m-\frac{N}{2}}
\end{aligned}$$

Next, we use a similar procedure to replace the term  $r_{2,N}(w)$  in the double contour integrals. We need an expansion of  $r_{2,N}(w)$  in terms of the eigenvalues  $r_{\alpha,2}(w)$  and  $r_{\beta,2}(w)$ , which we state below.

**Lemma 3.6.** *Let  $\delta = \max\{\alpha, \beta\}$  and let  $\mathcal{B} = (-\infty, -\delta^{-2}] \cup [-\delta^2, 0]$ .<sup>6</sup> For  $z \in \mathbb{C} \setminus \mathcal{B}$  and  $N$  sufficiently large the following expansion converges,*

$$(50) \quad r_{2,N}(z) = \sum_{p=0}^{\infty} \sum_{q=0}^{\infty} c_{p,q}(z) r_{\alpha,2}(z)^{\frac{(2p+1)N}{2}} r_{\beta,2}(z)^{\frac{(2q+1)N}{2}}$$

Where the coefficients  $c_{p,q}(z)$  are non-singular and non-zero at  $z = 1$ .

The proof of Lemma 3.6 is in Section 6. It is important to check that the coefficients of the above series do not affect the pole at  $w = 1$ , but besides that, the exact statement of the coefficients is mostly unimportant. The only coefficient we need, and thus state explicitly, is

$$(51) \quad c_{0,0}(w) = \frac{2}{1 + 2g_{\alpha,\beta}(w)}$$

When we plug this expansion into the double contour integrals, most of the terms evaluate to zero due to the residue theorem. To see this, first consider the product

$$\frac{1}{(w-1)^N} f(w) r_{\alpha,1}(w)^{N-m'} r_{\beta,1}(w)^{\frac{N}{2}}$$

This has no pole at  $w = 1$  as long as  $f(w)$  has a zero at  $w = 1$  that is at least of order  $4N$ . Similarly, the product

$$\frac{1}{(w-1)^N} f(w) r_{\alpha,1}(w)^{m'} r_{\beta,1}(w)^{\frac{N}{2}}$$

has no pole at  $w = 1$  as long as  $f(w)$  has a zero at  $w = 1$  of at least order  $3N$ . This leaves us with the following simplification of the correlation kernel,

$$\begin{aligned}
(52) \quad & \left[ \mathbb{K}_N(4m', 2\xi' + j; 4m, 2\xi + i) \right]_{i,j=0}^1 = -\frac{\mathbb{I}_{m>m'}}{2\pi i} \oint_{\gamma_{0,1}} \frac{dz}{z} z^{\xi'-\xi} \Phi_\alpha(z)^{\frac{N}{2}-m'} \Phi_\varepsilon(z)^{m-\frac{N}{2}} \\
& + \frac{1}{(2\pi i)^2} \oint_{\gamma_1} dw \oint_{\gamma_{0,1}} \frac{dz}{z(z-w)} \frac{w^{\xi'+N}(z-1)^N}{z^{\xi+N}(w-1)^N} r_{\alpha,1}(w)^{\frac{N}{2}-m'} \frac{2F_{\alpha,1}(w)F_{\beta,1}(w)F_{\alpha,1}(w)}{1+2g(w)} \Phi_\varepsilon(z)^{m-\frac{N}{2}} \\
& + \frac{1}{(2\pi i)^2} \oint_{\gamma_1} dw \oint_{\gamma_{0,1}} \frac{dz}{z(z-w)} \frac{w^{\xi'+N}(z-1)^N}{z^{\xi+N}(w-1)^N} r_{\alpha,2}(w)^{\frac{N}{2}-m'} \frac{2F_{\alpha,2}(w)F_{\beta,1}(w)F_{\alpha,1}(w)}{1+2g_{\alpha,\beta}(w)} \Phi_\varepsilon(z)^{m-\frac{N}{2}}
\end{aligned}$$

<sup>6</sup>We let  $\mathcal{B}$  denote the larger of the possible branch cuts.

To obtain the final form we first notice that

$$(53) \quad \frac{2F_{\alpha,1}(w)F_{\beta,1}(w)F_{\alpha,1}(w)}{1+2g(w)} = F_{\alpha,1}(w)$$

**3.3. Proof of Theorem 2.1 when  $N/2 < m' < N$ .** To prove Theorem 2.1 for  $m' > N/2$ , we follow a similar procedure to the case when  $m' < N/2$ . We first expand the double contour integral using eigen-decompositions of  $\Phi_\alpha(w)$  and  $\Phi_\beta(w)$ . Then we simplify the  $w$ -integral by replacing the matrix products  $F_{\beta,1}(w)F_{1,N}(w)$  and  $F_{\beta,2}(w)F_{1,N}(w)$  with the expressions given in equations (41) and (42). Lastly, we use Lemma 3.6 to replace the term  $r_{2,N}(w)$ . The differences are in the details, which we will highlight below. First, we state the expanded version of the kernel,

$$(54) \quad \left[ \mathbb{K}_N(4m', 2\xi' + j; 4m, 2\xi + i) \right]_{i,j=0}^1 = -\frac{\mathbb{I}_{m>m'}}{2\pi i} \oint_{\gamma_{0,1}} \frac{dz}{z} z^{\xi'-\xi} \Phi_\alpha(z)^{\frac{N}{2}-m'} \Phi_\varepsilon(z)^{m-\frac{N}{2}}$$

$$+ \frac{1}{(2\pi i)^2} \sum_{k_1=1,2} \sum_{k_2=1,2} \sum_{k_3=1,2} \oint_{\gamma_1} \oint_{\gamma_{0,1}} \frac{dw dz}{z(z-w)} \frac{w^{\xi'+N}(z-1)^N}{z^{\xi+N}(w-1)^N} r_{\beta,k_1}(w)^{\frac{N}{2}-m'} r_{\alpha,k_2}(w)^{-\frac{N}{2}} r_{\alpha,k_3}(w)^{\frac{N}{2}}$$

$$\times F_{\beta,k_1}(w)F_{\alpha,k_2}(w)F_{1,N}(w)F_{\alpha,k_3}(w)\Phi_\varepsilon(z)^{m-\frac{N}{2}}$$

Again our goal will be to track count the order of the pole/zero at  $w = 1$ . The term

$$\frac{1}{(w-1)^N} r_{\beta,k_1}(w)^{\frac{N}{2}-m'} r_{\alpha,k_2}(w)^{-\frac{N}{2}} r_{\alpha,k_3}(w)^{\frac{N}{2}}$$

considers all the parts of the integral, besides  $F_{1,N}(w)$ , that potentially contribute to the pole at  $w = 1$ . Depending on the value of  $k_1$ ,  $k_2$ , and  $k_3$  the order of the pole (or zero) differs. We first track the highest possible pole order (or lowest possible zero order) when  $k_2 = 1$ ,

	$k_1 = 1$	$k_1 = 2$
$k_3 = 1$	pole of order $< N$	pole of order $< 2N$
$k_3 = 2$	zero of order $> N$	zero of order $> 0$

Next we do the same procedure, assuming  $k_2 = 2$ ,

	$k_1 = 1$	$k_1 = 2$
$k_3 = 1$	pole of order $< 3N$	pole of order $< 4N$
$k_3 = 2$	pole of order $< N$	pole of order $< 2N$

We are now ready to replace the terms  $F_{\alpha,k_2}(w)F_{1,N}(w)$  by using either equation (41) or equation (42). We are careful to observe which terms actually have a pole at  $w = 1$ . As was the case in Section 3.2, many of the terms drop out of the contour integral as a result of the residue theorem.

We simplify the original double contour integrals down to four integrals,

$$\begin{aligned}
(55) \quad & \sum_{k_1=1,2} \sum_{k_2=1,2} \sum_{k_3=1,2} \oint_{\gamma_1} \oint_{\gamma_{0,1}} \frac{dw dz}{z(z-w)} \frac{w^{\xi'+N}(z-1)^N}{z^{\xi+N}(w-1)^N} r_{\beta,k_1}(w)^{\frac{N}{2}-m'} r_{\alpha,k_2}(w)^{-\frac{N}{2}} r_{\alpha,k_3}(w)^{\frac{N}{2}} \\
& \quad \times F_{\beta,k_1}(w) F_{\alpha,k_2}(w) F_{1,N}(w) F_{\alpha,k_3}(z) \Phi_\varepsilon(z)^{m-\frac{N}{2}} \\
& = \sum_{k=1,2} \oint_{\gamma_1} \oint_{\gamma_{0,1}} \frac{dw dz}{z(z-w)} \frac{w^{\xi'+N}(z-1)^N}{z^{\xi+N}(w-1)^N} r_{\beta,k}(w)^{\frac{N}{2}-m'} r_{2,N}(w) r_{\alpha,1}(w)^{\frac{N}{2}} r_{\beta,1}(w)^{\frac{N}{2}} \\
& \quad \times F_{\beta,k}(w) F_{\alpha,1}(w) F_{\beta,1}(w) F_{\alpha,1}(w) \Phi_\varepsilon(z)^{m-\frac{N}{2}} \\
& + \sum_{k=1,2} \oint_{\gamma_1} \oint_{\gamma_{0,1}} \frac{dw dz}{z(z-w)} \frac{w^{\xi'+N}(z-1)^N}{z^{\xi+N}(w-1)^N} r_{\beta,k}(w)^{\frac{N}{2}-m'} r_{\alpha,1}(w)^{\frac{N}{2}} r_{2,N}(w) r_{\beta,1}(w)^{\frac{N}{2}} \\
& \quad \times F_{\beta,k}(w) F_{\alpha,2}(w) F_{\beta,1}(w) F_{\alpha,1}(w) \Phi_\varepsilon(z)^{m-\frac{N}{2}}
\end{aligned}$$

The first sum of integrals and second sum of integrals can be combined, by matching up the integrals with the same value of  $k$ . In particular, we get

$$\begin{aligned}
& F_{\beta,k}(w) F_{\alpha,1}(w) F_{\beta,1}(w) F_{\alpha,1}(w) \Phi_\varepsilon(z)^{m-\frac{N}{2}} + F_{\beta,k}(w) F_{\alpha,2}(w) F_{\beta,1}(w) F_{\alpha,1}(w) \Phi_\varepsilon(z)^{m-\frac{N}{2}} \\
& = F_{\beta,k}(w) \left( F_{\alpha,1}(w) + F_{\alpha,2}(w) \right) F_{\beta,1}(w) F_{\alpha,1}(w) \Phi_\varepsilon(z)^{m-\frac{N}{2}} \\
& = F_{\beta,k}(w) F_{\beta,1}(w) F_{\alpha,1}(w) \Phi_\varepsilon(z)^{m-\frac{N}{2}}
\end{aligned}$$

This simplification show that when  $k = 2$ , the matrix product is zero due to the orthogonality of the  $F_\beta$ -matrices. Thus we are left with only one double contour integral,

$$(56) \quad \oint_{\gamma_1} \oint_{\gamma_{0,1}} \frac{dw dz}{z(z-w)} \frac{w^{\xi'+N}(z-1)^N}{z^{\xi+N}(w-1)^N} r_{\beta,1}(w)^{N-m'} r_{2,N}(w) r_{\alpha,1}(w)^{\frac{N}{2}} F_{\beta,1}(w) F_{\alpha,1}(w) \Phi_\varepsilon(z)^{m-\frac{N}{2}}$$

We are now ready to apply Lemma 3.6. Notice that the product  $(w-1)^{-N} r_{\beta,1}(w)^{N-m'} r_{\alpha,1}(w)^{\frac{N}{2}}$  has a pole at  $w = 1$  of order less than  $3N$ . This means that only the first term of the expansion in Lemma 3.6 contributes non-trivially to the integral. The double contour integral in (56) then becomes,

$$(57) \quad \oint_{\gamma_1} \oint_{\gamma_{0,1}} \frac{dw dz}{z(z-w)} \frac{w^{\xi'+N}(z-1)^N}{z^{\xi+N}(w-1)^N} r_{\beta,1}(w)^{\frac{N}{2}-m'} \frac{2}{1+2g_{\alpha,\beta}(w)} F_{\beta,1}(w) F_{\alpha,1}(w) \Phi_\varepsilon(z)^{m-\frac{N}{2}}$$

Applying this double contour integral into the formula in (54), yields the expression presented in equation (16).

**3.4. Proof of Corollary 2.1.** We have two goals in mind for wanting to prove Corollary 2.1. Firstly, the kernels on the  $\alpha$ -side and  $\beta$ -side of the interface now have a symmetry to them and we are free to limit our computations by looking at a single side of the model.<sup>7</sup> Secondly, the adjusted form of the kernel contains the correlation kernel for the typically two-periodic Aztec diamond, so we will more easily be able to make comparisons.

<sup>7</sup>In the case of the typical two-periodic Aztec diamond, this kernel symmetry is obvious by flipping the Aztec diamond twice (vertically and horizontally) and then gauge transforming the edge weights. In the case of the split two-periodic model, you can no longer use a gauge transformation to get back to the original edge weights as the interface causes a problem.

The main process we take in this proof is move the  $w$ -contour of the double contour integral to the branch cuts and then through the branch cuts on to the second sheet of the Riemann surface that was described earlier in Section 2.3.

*Proof.* We start with the form of the kernel presented in equation (16). We make the following observations about the  $F$ -matrices,

$$(58) \quad \frac{2}{1+2g_{\alpha,\beta}(w)}F_{\beta,1}(w)F_{\alpha,1}(w) = F_{\beta,1}(w) - \frac{2}{1+2g_{\alpha,\beta}(w)}F_{\beta,1}(w)F_{\alpha,2}(w)F_{\beta,2}(w)$$

Next, we substitute this equality into the double contour integral in equation (16). We write the result as two separate contour integrals,

$$(59) \quad \oint_{\gamma_1} \oint_{\gamma_{0,1}} \frac{dw dz}{z(z-w)} \frac{w^{\xi'+N}(z-1)^N}{z^{\xi+N}(w-1)^N} r_{\beta,1}(w)^{\frac{N}{2}-m'} \frac{2}{1+2g_{\alpha,\beta}(w)} F_{\beta,1}(w) F_{\alpha,1}(w) \Phi_\varepsilon(z)^{m-\frac{N}{2}}$$

$$= \oint_{\gamma_1} \oint_{\gamma_{0,1}} \frac{dw dz}{z(z-w)} \frac{w^{\xi'+N}(z-1)^N}{z^{\xi+N}(w-1)^N} r_{\beta,1}(w)^{\frac{N}{2}-m'} F_{\beta,1}(w) \Phi_\varepsilon(z)^{m-\frac{N}{2}}$$

$$- \oint_{\gamma_1} \oint_{\gamma_{0,1}} \frac{dw dz}{z(z-w)} \frac{w^{\xi'+N}(z-1)^N}{z^{\xi+N}(w-1)^N} r_{\beta,1}(w)^{\frac{N}{2}-m'} \frac{2F_{\beta,1}(w)F_{\alpha,2}(w)F_{\beta,2}(w)}{1+2g_{\alpha,\beta}(w)} \Phi_\varepsilon(z)^{m-\frac{N}{2}}$$

The first double contour integral matches up with the first double contour integral in (15), so we do not need to manipulate it further.

We set the branch cuts of the  $w$  part of the second double contour integral to be along the negative real axis. Let  $\delta = \max\{\alpha, \beta\}$ , then the branch cuts are  $(-\infty, -\delta^{-2}] \cup [-\delta^2, 0]$ . We deform the contour  $\gamma_1$  out to infinity and around, so that the new contour surrounds only the branch cuts. From this maneuver, we get an additional single contour integral residue at  $z = w$ . This single contour integral has the form,

$$\oint_{\gamma_{0,1}} \frac{dz}{z} z^{\xi'-\xi} r_{\beta,1}(z)^{\frac{N}{2}-m'} \frac{2F_{\beta,1}(z)F_{\alpha,2}(z)F_{\beta,2}(z)}{1+2g_{\alpha,\beta}(z)} \Phi_\varepsilon(z)^{m-\frac{N}{2}}$$

Next we will pass the  $w$  contour of the double contour integral through the branch cuts and on to the second sheet of the Riemann surface. Pushing the contour to the other sheet means we need to make the following changes to the integral:  $r_{\beta,1}(w) \rightarrow r_{\beta,2}(w)$  and

$$\frac{2}{1+2g_{\alpha,\beta}(w)}F_{\beta,1}(w)F_{\alpha,2}(w)F_{\beta,2}(w) \rightarrow \frac{2}{1+2g_{\alpha,\beta}(w)}F_{\beta,2}(w)F_{\alpha,1}(w)F_{\beta,1}(w)$$

These are the analytic continuations of the functions on the other sheet. Also, pushing the contour through to the second sheet changes the direction of the contour, introducing a minus sign. We have thus shown,

$$(60) \quad - \oint_{\gamma_1} \oint_{\gamma_{0,1}} \frac{dw dz}{z(z-w)} \frac{w^{\xi'+N}(z-1)^N}{z^{\xi+N}(w-1)^N} r_{\beta,1}(w)^{\frac{N}{2}-m'} \frac{2F_{\beta,1}(w)F_{\alpha,2}(w)F_{\beta,2}(w)}{1+2g_{\alpha,\beta}(w)} \Phi_\varepsilon(z)^{m-\frac{N}{2}}$$

$$= \oint_{\gamma_{\text{Br}}} \oint_{\gamma_{0,1}} \frac{dw dz}{z(z-w)} \frac{w^{\xi'+N}(z-1)^N}{z^{\xi+N}(w-1)^N} r_{\beta,2}(w)^{\frac{N}{2}-m'} \frac{2F_{\beta,2}(w)F_{\alpha,1}(w)F_{\beta,1}(w)}{1+2g_{\alpha,\beta}(w)} \Phi_\varepsilon(z)^{m-\frac{N}{2}}$$

$$+ \frac{1}{2\pi i} \oint_{\gamma_{0,1}} \frac{dz}{z} z^{\xi'-\xi} r_{\beta,1}(z)^{\frac{N}{2}-m'} \frac{2F_{\beta,1}(z)F_{\alpha,2}(z)F_{\beta,2}(z)}{1+2g_{\alpha,\beta}(z)} \Phi_\varepsilon(z)^{m-\frac{N}{2}}$$

Where  $\gamma_{\text{Br}}$  denotes the contour surround the branch cuts (in the clockwise direction). When we deform the contour  $\gamma_{\text{Br}}$  back to  $\gamma_1$ , we once again pick up another single integral term,

$$(61) = \oint_{\gamma_1} \oint_{\gamma_{0,1}} \frac{dw dz}{z(z-w)} \frac{w^{\xi'+N}(z-1)^N}{z^{\xi+N}(w-1)^N} r_{\beta,2}(w)^{\frac{N}{2}-m'} \frac{2F_{\beta,2}(w)F_{\alpha,1}(w)F_{\beta,1}(w)}{1+2g_{\alpha,\beta}(w)} \Phi_\varepsilon(z)^{m-\frac{N}{2}} \\ - \frac{1}{2\pi i} \oint_{\gamma_{0,1}} \frac{dz}{z} z^{\xi'-\xi} r_{\beta,2}(z)^{\frac{N}{2}-m'} \frac{2F_{\beta,2}(z)F_{\alpha,1}(z)F_{\beta,1}(z)}{1+2g_{\alpha,\beta}(z)} \Phi_\varepsilon(z)^{m-\frac{N}{2}} \\ - \frac{1}{2\pi i} \oint_{\gamma_{0,1}} \frac{dz}{z} z^{\xi'-\xi} r_{\beta,1}(z)^{\frac{N}{2}-m'} \frac{2F_{\beta,1}(z)F_{\alpha,2}(z)F_{\beta,2}(z)}{1+2g_{\alpha,\beta}(z)} \Phi_\varepsilon(z)^{m-\frac{N}{2}}$$

The two single integrals end up canceling out via the same procedure just described (e.g. for one of the integrals, push the contour through the branch cut to the other sheet). Now we have obtained the results presented in Corollary 2.1.  $\square$

#### 4. LOCAL ASYMPTOTICS OF THE MODEL

The goal of this section is to prove the local asymptotic results stated in Propositions 2.1 and 2.2. We begin in Section 4.1 by stating some necessary results about the behavior of the saddle functions. In particular, we need precise statements about the location of saddle points and the contours of steepest ascent and descent in the smooth and rough regions of the model. Once we have the necessary preliminary information, we prove Propositions 2.1 and 2.2 in Sections 4.2 and 4.3, respectively.

**4.1. Preliminaries of Saddle Functions.** Recall the piece-wise definition of the saddle function  $\psi_k(z)$ ,

$$(62) \quad \psi_k(z; x, y) = \begin{cases} \psi_{\alpha,k}(z; x, y) & \text{for } x < 1/2 \\ \psi_{\beta,k}(z; x, y) & \text{for } x > 1/2 \end{cases}$$

where  $\psi_{\varepsilon,k}(z)$  is defined in equation (21). We start by stating a basic lemma regarding the asymptotic behavior of the function  $\text{Re } \psi_k(z)$ .

**Lemma 4.1.** *As  $z \rightarrow \infty$ , the saddle functions exhibit the following asymptotic behavior,*

$$\text{Re } \psi_k(z) = y \log |z| + O(1)$$

*Proof.* One can observe from the definition of  $r_{\varepsilon,1}(z)$  and  $r_{\varepsilon,2}(z)$  that

$$\lim_{z \rightarrow \infty} r_{\varepsilon,k}(z) = 1$$

for  $k = 1, 2$ . Also, as  $z \rightarrow \infty$  we have,

$$(y+1) \log |z| - \log |z-1| = y \log |z| + O(z^{-1})$$

$\square$

A direct consequence of this lemma is that for any  $(x, y) \in (0, 1) \times (-1, 0)$ ,  $\text{Re } \psi_k(z) \rightarrow -\infty$  as  $z \rightarrow \infty$ .

We know that  $\psi_k(z)$  always has at least one saddle point between the branch cuts on the negative real axis. We denote this saddle point  $z_k^*$ .<sup>8</sup> We start by stating,

**Lemma 4.2.** *For any  $(x, y) \in (0, 1/2) \times (-1, 0)$ , the following is true regarding the saddle point  $z_k^*$*

- (i)  $z_2^*$  is a local maximum,

<sup>8</sup>This is the same notation used in [11].

(ii) if  $(x, y) \in \mathfrak{S}$ , then  $z_1^*$  is a local maximum, otherwise it is a local minimum.

This is largely a subset of Lemma 6.8 in [11]. There are a few key differences we take the time to acknowledge and justify. Firstly, since there is an overall sign change between their saddle function and the saddle function presented here, there is a reversal of maxima and minima. Additionally, while the asymptotic coordinate is restricted to the smooth region in the proof presented by Duits and Kuijlaars, we address cases where this is not necessarily true. We present the proof of these additional part below.

*Proof.* Assume that  $(x, y) \in \mathfrak{F} \cup \mathfrak{R}$  in addition to the fact that  $x < 1/2$ . In this case, there is exactly one saddle point of  $\psi_k(z)$  on the interval  $(-\alpha^{-2}, -\alpha^2)$ . We consider the behavior of  $\text{Re } \psi'_k(z)$  as we approach the branch points. In particular, we have

$$(63) \quad \lim_{z \rightarrow (-\alpha^2)^-} \frac{r'_{\alpha,1}(z)}{r_{\alpha,1}(z)} = +\infty \quad \lim_{z \rightarrow (-\alpha^{-2})^+} \frac{r'_{\alpha,1}(z)}{r_{\alpha,1}(z)} = -\infty$$

$$(64) \quad \lim_{z \rightarrow (-\alpha^2)^-} \frac{r'_{\alpha,2}(z)}{r_{\alpha,2}(z)} = -\infty \quad \lim_{z \rightarrow (-\alpha^{-2})^+} \frac{r'_{\alpha,2}(z)}{r_{\alpha,2}(z)} = +\infty$$

From this we deduce that  $z_2^*$  is a local maximum of  $\text{Re } \psi_2(z)$  and  $z_1^*$  is a local minimum of  $\text{Re } \psi_1(z)$ .  $\square$

The *contour of steepest ascent* from  $z_k^*$  is the contour through  $z_k^*$  where  $\text{Im } \psi_k(z)$  is held constant and  $\text{Re } \psi_k(z)$  increases the fastest as we move away from the saddle point. Since  $z_2^*$  is a maximum of  $\text{Re } \psi_2(z)$ , the path of steepest ascent is perpendicular to the real axis at  $z_2^*$  (the same is true for  $z_1^*$  when the asymptotic coordinate is in the smooth region). We define the following regions of the plane,<sup>9</sup>

$$(65) \quad \Omega_k^+ = \{z \in \mathbb{C} : \text{Re } \psi_k(z) > \text{Re } \psi_k(z_k^*)\}$$

$$(66) \quad \Omega_k^- = \{z \in \mathbb{C} : \text{Re } \psi_k(z) < \text{Re } \psi_k(z_k^*)\}$$

Now we state the following lemma,

**Lemma 4.3.** *For any  $(x, y) \in (0, 1/2) \times (-1, 0)$  the following holds,*

- (i) *The steepest ascent contour of  $\psi_2(z; x, y)$  through  $z_2^*$ , denoted  $\gamma_{s,2}$ , is a simple closed curve that contains the interval  $[-\alpha^2, 0]$  and intersects the positive real line at  $z = 1$ .*
- (ii)  *$\Omega_2^+$  is a bounded set containing a single component which contains  $\gamma_{s,2} \setminus \{z_2^*\}$ .*
- (iii)  *$\Omega_2^-$  is an open set with an unbounded component that contains a contour going around  $(-\infty, -\alpha^{-2}]$  and with a bounded component that contains a contour around  $[-\alpha^2, 0]$ .*

*Under the additional condition that  $(x, y) \in \mathfrak{S}$ , the following also holds*

- (i) *The steepest ascent contour of  $\psi_1(z; x, y)$  through  $z_1^*$ , denoted  $\gamma_{s,1}$ , is a simple closed curve that contains the interval  $[-\alpha^2, 0]$  and intersects the positive real line at  $z = 1$ .*
- (ii)  *$\Omega_1^+$  is a bounded set containing at most three components which contains  $\gamma_{s,1} \setminus \{z_1^*\}$ .*
- (iii)  *$\Omega_1^-$  is an open set with an unbounded component that contains a contour going around  $(-\infty, -\alpha^{-2}]$  and with a bounded component that contains a contour around  $[-\alpha^2, 0]$ .*

Figure 9 shows an example of the regions  $\Omega_2^+$  and  $\Omega_2^-$  along with the steepest ascent contour. This lemma is a slightly modified version of Lemma 6.9 of [11]. The reader should refer to their text for a the proof. Note that the proof given also holds for  $\psi_2(z)$  as long as the asymptotic coordinate of the model is to the left of the interface (and regardless of the macroscopic region of the model).

<sup>9</sup>While this notation is the same as in [11] the regions will be reversed in our notation due to the change in sign of the saddle functions presented here.

In the first part, we conclude that  $\Omega_2^+$  is a single component, because there is exactly one saddle point on the interval  $(-\alpha^{-2}, -\alpha^2)$ .

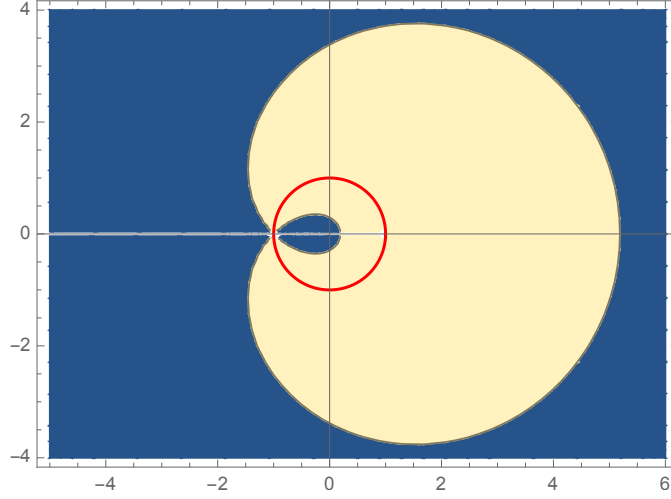


FIGURE 9. An example of the steepest ascent contour of  $\psi_2(z; x, y)$  through  $z_2^*$  and the regions  $\Omega_2^+$  and  $\Omega_2^-$ . The steepest ascent contour is shown in red,  $\Omega_2^+$  is the region in yellow, and  $\Omega_2^-$  is the region in blue. Contour plot was generated with Mathematica.

The above information is enough for the analysis of  $I_{2,2}^\alpha$  and for the analysis of  $I_{2,1}^\alpha$  in the smooth region. In order to analyze  $I_{2,1}^\alpha$  in the rough region, we will need some information on the contours of steepest descent and ascent in the rough region. For  $x \in (0, 1/2)$  and  $(x, y) \in \mathfrak{R}$ , the saddle function  $\psi_1(z)$  has three saddle point,  $z_1^*$ ,  $z_3^*$ , and  $z_4^*$ , where the latter two are complex. In particular,  $z_3^* = \overline{z_4^*}$ . Let  $z_3^*$  denote the complex saddle point with positive imaginary part. We define the following regions of the complex plane,

$$(67) \quad \Pi^+ = \{z \in \mathbb{C} : \operatorname{Re} \psi_1(z) > \operatorname{Re} \psi_1(z_3^*)\}$$

$$(68) \quad \Pi^- = \{z \in \mathbb{C} : \operatorname{Re} \psi_1(z) < \operatorname{Re} \psi_1(z_3^*)\}$$

It suffices to define these regions just using  $z_3^*$ , since  $\operatorname{Re} \psi_1(z_3^*) = \operatorname{Re} \psi_1(z_4^*)$ . We now describe some important aspects about these regions,

**Lemma 4.4.** *Let  $(x, y) \in \mathfrak{R}$  and  $x \in (0, 1/2)$ , then*

- (i)  $\Pi^+$  contains at least two and at most three bounded components. One component will always contain  $z = 1$ , while the other guaranteed component contains at least one of the branch points,  $-\alpha^2$  or  $-\alpha^{-2}$ . The third component, if it exists, must contain the other branch point, intersect the branch cut, and be positive distance away from the other components.
- (ii)  $\Pi^-$  contains a bounded component, which contains  $z = 0$ , and an unbounded component.

*Proof.* We will focus only on the upper half plane, since the regions  $\Pi^\pm$  are symmetric about the real axis. The boundary between these regions are contours where  $\operatorname{Re} \psi_1(z) = \operatorname{Re} \psi_1(z_3^*)$ . These contours remain bounded, since  $\operatorname{Re} \psi_1(z) \rightarrow -\infty$  as  $z \rightarrow \infty$ . Additionally, these contours do not intersect anywhere in the upper half plane or on the real axis, because this would violate the maximum principle of harmonic functions. This means that the four half-paths emanating from  $z_3^*$  intersect the real axis at four different points. To see the possible intersection points, we note the following limits,



- $\lim_{z \rightarrow \infty} \operatorname{Re} \psi_1(z) = -\infty$
- $\lim_{z \rightarrow 0} \operatorname{Re} \psi_1(z) = -\infty$
- $\lim_{z \rightarrow 1} \operatorname{Re} \psi_1(z) = +\infty$

We also have the following behavior on intervals,

- $\operatorname{Re} \psi_1(z)$  is strictly decreasing on  $(1, \infty)$
- $\operatorname{Re} \psi_1(z)$  is strictly increasing on  $(0, 1)$
- $\operatorname{Re} \psi_1(z)$  is strictly increasing on  $(-\infty, -\alpha^{-2})$
- $\operatorname{Re} \psi_1(z)$  is strictly decreasing on  $(-\alpha^2, z_1^*)$
- $\operatorname{Re} \psi_1(z)$  is strictly increasing on  $(z_1^*, -\alpha^2)$
- $\operatorname{Re} \psi_1(z)$  is strictly decreasing on  $(-\alpha^2, 0)$

This means that one half-path intersects the real axis at some value greater than one and one half-path intersects the real axis on the interval  $(0, 1)$ . The other two half paths should intersect the negative real axis. It is clear from the limits that  $\Pi^+$  should contain the point  $z = 1$ ,  $\Pi^-$  should contain the point  $z = 0$ , and that  $\Pi^-$  should contain an unbounded component.

Since  $\operatorname{Re} \psi_1(z)$  is not strictly increasing on the interval  $(-\infty, 0)$ , where the two half-paths intersect this interval can vary. Either  $-\alpha^2$  or  $-\alpha^{-2}$  is a global maximum of  $\operatorname{Re} \psi_1(z)$  on  $(-\infty, 0)$ , so at least one of them (possibly both) must be contained in  $\Pi^+$ . Alternatively, one of the branch points may be contained in a separate third component that intersect the branch cut.<sup>10</sup> There can only be one additional component since any additional components must intersect the branch cuts and  $\operatorname{Re} \psi_1(x)$  is monotonic along the branch cuts. Similarly, there is no additional component of  $\Pi^-$  because it would have to be away from the branch cuts and thus it would break the maximum/minimum principle of harmonic functions.  $\square$

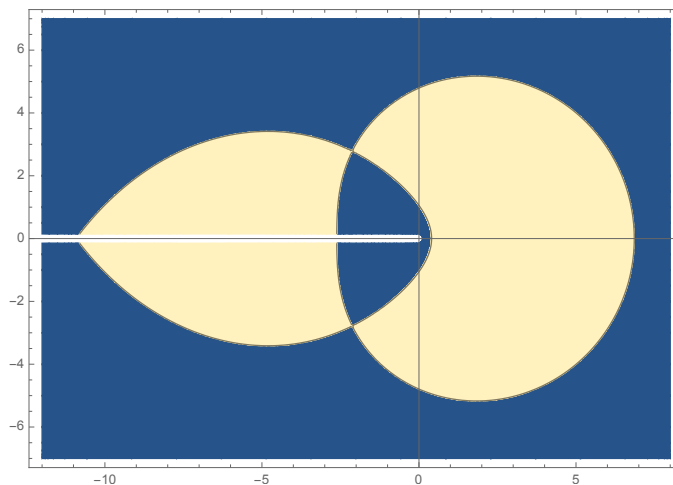


FIGURE 10. An example of the regions  $\Pi^\pm$  for  $(x, y) \in \mathfrak{R}$ ,  $\Pi^-$  is the region in blue while  $\Pi^+$  is the region in yellow. Contour plot was generated in Mathematica.

An example of the regions  $\Pi^\pm$  are shown in Figure 10. Since we know the contours of steepest ascent and descent through  $z_3^*$  and  $z_4^*$  should lie entirely in  $\Pi^+ \setminus \{z_3^*, z_4^*\}$  and  $\Pi^- \setminus \{z_3^*, z_4^*\}$ , respectively, understanding these regions gives us enough information to understand the contours. We let  $\gamma_{R,A}$  denote the contour of steepest ascent and we let  $\gamma_{R,D}$  denote the contour of steepest descent. An example of these contours is given in Figure 11.

<sup>10</sup>It is unclear whether this actually occurs, but it does not affect our analysis either way.

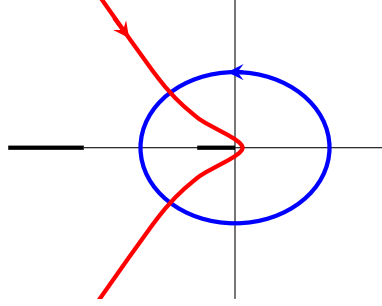


FIGURE 11. Steepest descent and ascent contours for  $\psi_1(z)$  in the rough region. The point where the contours cross are the two complex saddle points. The red contour is the path of steepest descent, while the blue contour is the path of steepest ascent.

4.2. **Asymptotics of  $I_{2,2}^\alpha$ .** The goal of this section is to prove Proposition 2.1. As we can see from the statement, the proof depends on the relative magnitudes of  $\alpha$  and  $\beta$ . This is because the branch cuts of the integral in  $I_{2,2}^\alpha$  are different in the cases of  $\beta < \alpha$  and  $\alpha < \beta$ . In the case of  $\beta < \alpha$  the branch cuts are  $(-\infty, -\alpha^{-2}] \cup [-\alpha^2, 0]$ . Alternately, if  $\alpha < \beta$  the branch cuts are  $(-\infty, -\beta^{-2}] \cup [-\beta^2, 0]$ . These branch cuts are depicted in Figure 12. We begin by proving the former case.

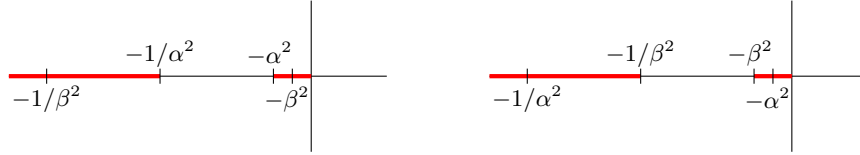


FIGURE 12. Branch cuts of the  $w$ -integral part of the integral in  $I_{2,2}^\alpha$ . The left hand image shows the branch cuts when  $0 < \beta < \alpha < 1$ , while the right hand image shows the branch cuts when  $0 < \alpha < \beta < 1$ . Note the left most branch cuts go off to infinity in both images.

4.2.1. *Asymptotics on the  $\alpha$ -side when  $\beta < \alpha$ .* Here we will prove the statement regarding  $I_{2,2}^\alpha$  in Proposition 2.1 under the condition  $0 < \beta < \alpha < 1$ .

*Proof.* We start with the definition of  $[I_{2,2}^\alpha(4m', 2\xi' + j; 4m, 2\xi + i)]_{i,j=0}^1$  presented in equation 27. Next, deform the  $w$ -contour so it will ultimately surround the branch cuts, which are depicted in Figure 12. We do so by pushing the  $w$ -contour to infinity, and then flipping it around so it surrounds the negative real axis. We shrink the contour to just around the branch cuts. Where there is not a branch cut along the negative real axis, the contours cancel out. We are left with two separate contours,  $\gamma_{w,1}$  and  $\gamma_{w,2}$ . We also deform the  $z$ -contour to the steepest ascent contour through the saddle point  $z_2^*$ . We refer to this contour as  $\gamma_{s,2}$  and it is described in Lemma 4.3. The resulting contours are depicted in Figure 13.

In deforming the contours we should be aware of the residue at  $z = w$  that results from crossing the contours, however this term drop out because of the matrix product that appears.

$$F_{\alpha,1}(z)F_{\alpha,2}(z) = 0$$

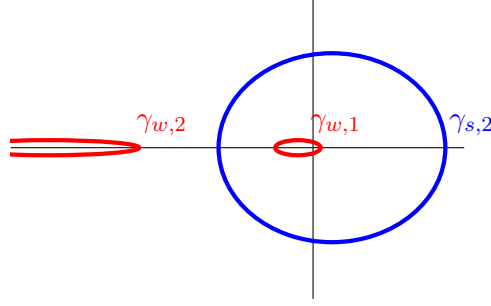


FIGURE 13. Depiction of the contours  $\gamma_{s,2}$ ,  $\gamma_{w,1}$ , and  $\gamma_{w,2}$  in the case of  $(x, y) \notin \mathfrak{C}$ .

Thus we are left with the equation,

$$(69) \quad \left[ I_{2,2}^\alpha(4m', 2\xi' + j; 4m, 2\xi + i) \right]_{i,j=0}^1 = \frac{1}{(2\pi i)^2} \oint_{\gamma_{w,1} \cup \gamma_{w,2}} \oint_{\gamma_{s,2}} \frac{dw dz}{z(z-w)} \frac{2F_{\alpha,2}(w)F_{\beta,1}(w)F_{\alpha,1}(w)}{1 + 2g_{\alpha,\beta}(w)} \\ \times F_{\alpha,2}(z) \exp [N(\psi_2(w; x, y) - \psi_2(z; x, y)) + \varphi_{\alpha,2}(w; x_2, y_2) - \varphi_{\alpha,2}(z; x_1, y_1)]$$

The function  $\varphi_{\alpha,2}(z)$  is defined back in equation 26. We are now ready to utilize saddle point asymptotics. As stated in Lemma 4.2 the saddle function  $\psi_2(z)$  always has one saddle point on the interval  $(-\alpha^{-2}, -\alpha^2)$ , which we refer to as  $z_2^*$ . The contours  $\gamma_{w,1}$  and  $\gamma_{w,2}$  not only lie away from the saddle point  $z_2^*$ , we can also guarantee that they both lie entirely inside of  $\Omega_2^-$  (per Lemma 4.3). Thus

$$(70) \quad \operatorname{Re} \psi_2(w; x, y) < \operatorname{Re} \psi_2(z_2^*; x, y) \leq \operatorname{Re} \psi_2(z; x, y)$$

for all  $w \in \gamma_{w,1} \cup \gamma_{w,2}$  and for all  $z \in \gamma_{s,2}$ . Moreover, Lemma 4.1 implies that as  $w \rightarrow \infty$ ,  $\operatorname{Re} \psi_2(w) \rightarrow -\infty$ . Combining these to statement mean that the term

$$\exp \left[ N(\psi_2(w; x, y) - \psi_2(z; x, y)) \right]$$

is  $O(e^{-cN})$  for some  $c > 0$ , uniformly for  $(z, w) \in \gamma_z \times \gamma_{w,1} \cup \gamma_{w,2}$ .  $\square$

4.2.2. *Asymptotics on the  $\alpha$ -side when  $\beta > \alpha$ .* We will utilize the following lemma when proving the local asymptotics of  $I_{2,2}^\alpha$  when  $\beta > \alpha$ . We state and prove the lemma below,

**Lemma 4.5.** *Let  $z^*$  be any complex number besides  $-\varepsilon^2$  and  $-\varepsilon^{-2}$ . Under the change of variables*

$$z - z^* = sN^{-1/2} \quad w - z^* = rN^{-1/2}$$

*we have the expansion,*

$$(71) \quad F_{\varepsilon,j}(w)F_{\varepsilon,k}(z) = N^{-1/2}F_{\varepsilon,j}(z^*)F'_{\varepsilon,k}(z^*)(s - r) + O(N^{-1})$$

*for  $j \neq k$ .*

*Proof.* To deal with this, we should expand these two matrix valued functions around the point  $z^*$ ,

$$F_{\varepsilon,1}(w) = F_{\varepsilon,1}(z^*) + F'_{\varepsilon,1}(z^*)(w - z^*) + O((w - z^*)^2) \\ F_{\varepsilon,2}(z) = F_{\varepsilon,2}(z^*) + F'_{\varepsilon,2}(z^*)(z - z^*) + O((z - z^*)^2)$$

The expansions are valid as long as we are away from the branch points. Applying the change of variable gives,

$$F_{\varepsilon,j}(w)F_{\varepsilon,k}(z) = N^{-1/2}F_{\varepsilon,j}(z^*)F'_{\varepsilon,k}(z^*)s + N^{-1/2}F'_{\varepsilon,j}(z^*)F_{\varepsilon,k}(z^*)r + O(N^{-1})$$

Lastly, one can check that

$$F_{\varepsilon,j}(z^*)F'_{\varepsilon,k}(z^*) = -F'_{\varepsilon,j}(z^*)F_{\varepsilon,k}(z^*)$$

yielding the results stated in the lemma.  $\square$

The local asymptotic behavior on the  $\alpha$ -side of the interface depends on where the saddle point  $z_2^*$  is located. Recall that  $z_2^*$  may be anywhere along the interval  $(-\alpha^{-2}, -\alpha^2)$  (we exclude the endpoints since these sit exactly on the interface). If  $z_2^* \in (-\beta^{-2}, -\beta^2)$ , then the proof is identical to the case in section 4.2.1 and the integral is  $O(e^{-N})$ . However, if the saddle point lies on one of the branch cuts, it is impossible for the  $w$ -contours to be entirely inside of  $\Omega_2^-$  as they were in Section 4.2.1. It is in these situations that our analysis differs.

Before we detail the proof of Proposition 2.1 in this case, we should first explain when our analysis fall into this category. Suppose  $z_2^* \in (-\alpha^{-2}, -\beta^{-2}]$ . Since  $z_2^*$  is the only maximum of  $\operatorname{Re} \psi_{\alpha,2}(z)$  (see Lemma 4.2) this implies that  $\psi'_{\alpha,2}(-\beta^{-2}; x, y) < 0$ . This inequality gives the following relationship between  $x$  and  $y$ ,

$$(72) \quad y < \frac{\beta^{-2}}{\beta^{-2} + 1} + \beta^{-2} \left( \frac{1}{2} - x \right) \log r_{\alpha,2}(-\beta^{-2})$$

Alternatively, supposing that  $z_2^* \in [-\beta^2, -\alpha^2)$  implies  $\psi'_{\alpha,2}(-\beta^2; x, y) > 0$ . This translates to the following inequality,

$$(73) \quad y > \frac{\beta^2}{\beta^2 + 1} + \beta^2 \left( \frac{1}{2} - x \right) \log r_{\alpha,2}(-\beta^2)$$

These inequalities describe the location of the strong-coupling region of the model. Examples of this region are given back in Figure 8. We are now prepared to consider the analysis of  $[I_{2,2}^\alpha(4m', 2\xi' + j; 4m, 2\xi + i)]_{i,j=0}^1$  when  $(x, y)$  satisfies one of the above inequalities.

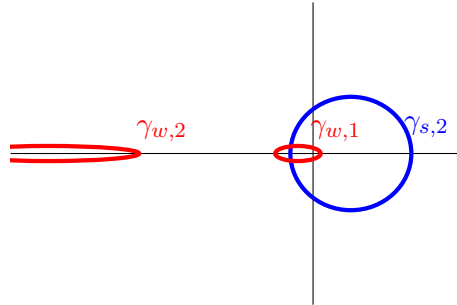


FIGURE 14. Depiction of the contours  $\gamma_{s,2}$ ,  $\gamma_{w,1}$ , and  $\gamma_{w,2}$  when  $(x, y) \in \mathfrak{C}$ .

*Proof of Proposition 2.1 for  $(x, y) \in \mathfrak{C}$ .* Assume  $z_2^* \in [-\beta^2, -\alpha^2)$ . We start by deforming the contours in the same way we did for the case of  $\beta < \alpha$ . Figure 14 gives an example of the contour deformation in this case. We split up the integral by the  $w$ -contours,

$$(74) \quad \begin{aligned} \left[ I_{2,2}^\alpha(4m', 2\xi' + j; 4m, 2\xi + i) \right]_{i,j=0}^1 &= \frac{1}{(2\pi i)^2} \oint_{\gamma_{w,1}} \oint_{\gamma_{s,2}} \frac{dw dz}{z(z-w)} \frac{2F_{\alpha,2}(w)F_{\beta,1}(w)F_{\alpha,1}(w)}{1 + 2g_{\alpha,\beta}(w)} \\ &\quad \times F_{\alpha,2}(z) \exp [N (\psi_2(w; x, y) - \psi_2(z; x, y)) + \varphi_{\alpha,2}(w; x_2, y_2) - \varphi_{\alpha,2}(z; x_1, y_1)] \\ &\quad + \frac{1}{(2\pi i)^2} \oint_{\gamma_{w,2}} \oint_{\gamma_{s,2}} \frac{dw dz}{z(z-w)} \frac{2F_{\alpha,2}(w)F_{\beta,1}(w)F_{\alpha,1}(w)}{1 + 2g_{\alpha,\beta}(w)} \\ &\quad \times F_{\alpha,2}(z) \exp [N (\psi_2(w; x, y) - \psi_2(z; x, y)) + \varphi_{\alpha,2}(w; x_2, y_2) - \varphi_{\alpha,2}(z; x_1, y_1)] \end{aligned}$$

Since  $\gamma_{w,2}$  still lies entirely inside of  $\Omega_2^-$ , we know that

$$\frac{1}{(2\pi i)^2} \oint_{\gamma_{w,2}} \oint_{\gamma_{s,2}} \frac{dw dz}{z(z-w)} \frac{2F_{\alpha,2}(w)F_{\beta,1}(w)F_{\alpha,1}(w)}{1+2g_{\alpha,\beta}(w)} F_{\alpha,2}(z) \\ \times \exp [N(\psi_2(w; x, y) - \psi_2(z; x, y)) + \varphi_{\alpha,2}(w; x_2, y_2) - \varphi_{\alpha,2}(z; x_1, y_1)]$$

is  $O(e^{-cN})$  for the same reasons as detailed in Section 4.2.1.

Now we separate the contour  $\gamma_{w,1}$  into two pieces:  $\gamma_{w,\uparrow}$ , which is the half lying above the real axis, and  $\gamma_{w,\downarrow}$ , which is the half lying below the real axis. We deform both of these contours to the negative real axis, which is the contour of steepest descent through  $z_2^*$ . We will start by just considering the contour integral

$$(75) \quad \frac{1}{(2\pi i)^2} \oint_{\gamma_{w,\uparrow}} \oint_{\gamma_{s,2}} \frac{dw dz}{z(z-w)} \frac{2F_{\alpha,2}(w)F_{\beta,1}(w)F_{\alpha,1}(w)}{1+2g_{\alpha,\beta}(w)} F_{\alpha,2}(z) \\ \times \exp [N(\psi_2(w; x, y) - \psi_2(z; x, y)) + \varphi_{\alpha,2}(w; x_2, y_2) - \varphi_{\alpha,2}(z; x_1, y_1)]$$

Expanding the saddle function  $\psi_2(z)$  around the saddle point  $z_2^*$  yields

$$(76) \quad \psi_2(z; x, y) = \psi_2(z_2^*) + \psi_2''(z_2^*)(z - z_2^*)^2 + O((z - z_2^*)^3)$$

Assuming we are away from the macroscopic boundaries, it follows that  $\psi_2''(z_2^*) \neq 0$ . Using the change of variables,

$$(77) \quad z - z_2^* = sN^{-1/2} \quad w - z_2^* = rN^{-1/2}$$

and the expansion in Lemma 4.5, we have

$$(78) \quad \frac{2F_{\alpha,2}(w)F_{\beta,1}(w)F_{\alpha,1}(w)F_{\alpha,2}(z)}{z(1+2g_{\alpha,\beta}(w))} = C_1 N^{-1/2}(s-r) + O(N^{-1})$$

where  $C_1$  is the matrix-valued constant,

$$(79) \quad C_1 = \frac{2F_{\alpha,2}(z_2^*)F_{\beta,1}(z_2^*)F_{\alpha,1}(z_2^*)F_{\alpha,2}'(z_2^*)}{z_2^*(1+2g_{\alpha,\beta}(z_2^*))}$$

Applying the change of variable given in equation (77) to the whole double contour integral yields,

$$(80) \quad \frac{1}{(2\pi i)^2} \oint_{\gamma_{w,\uparrow}} \oint_{\gamma_{s,1}} \frac{dw dz}{z(z-w)} \frac{2F_{\alpha,2}(w)F_{\beta,1}(w)F_{\alpha,1}(w)}{1+2g_{\alpha,\beta}(w)} F_{\alpha,2}(z) \\ \times \exp [N(\psi_2(w; x, y) - \psi_2(z; x, y)) + \varphi_{\alpha,2}(w; x_2, y_2) - \varphi_{\alpha,2}(z; x_1, y_1)] \\ = -C_1 \exp [\varphi_{\alpha,2}(z_2^*; x_2 - x_1, y_2 - y_1)] N^{-1} \int_{\mathbb{R}} dr \int_{i\mathbb{R}} ds \exp [\psi_2''(z_2^*)(r^2 - s^2)] + o(N^{-1})$$

By Lemma 4.2, we know that  $\text{Re } \psi_2''(z_2^*) < 0$ , since  $z_2^*$  is a maximum of  $\text{Re } \psi_2''(z)$ , and so the double integral is convergent. We repeat the procedure with the contour  $\gamma_{w,\downarrow}$ , noting that

$$(81) \quad \frac{2F_{\alpha,2}(w)F_{\beta,1}(w)F_{\alpha,1}(w)F_{\alpha,2}(z)}{z(1+2g_{\alpha,\beta}(w))} = \bar{C}_1 N^{-1/2}(s-r) + O(N^{-1})$$

since the contour has been deformed from below the branch cut. Thus we get,

$$(82) \quad \frac{1}{(2\pi i)^2} \oint_{\gamma_{w,\downarrow}} \oint_{\gamma_{s,1}} \frac{dw dz}{z(z-w)} \frac{2F_{\alpha,2}(w)F_{\beta,1}(w)F_{\alpha,1}(w)}{1+2g_{\alpha,\beta}(w)} F_{\alpha,2}(z) \\ \times \exp [N(\psi_2(w; x, y) - \psi_2(z; x, y)) + \varphi_{\alpha,2}(w; x_2, y_2) - \varphi_{\alpha,2}(z; x_1, y_1)] \\ = \bar{C}_1 \exp [\varphi_{\alpha,2}(z_2^*; x_2 - x_1, y_2 - y_1)] N^{-1} \int_{\mathbb{R}} dr \int_{i\mathbb{R}} ds \exp [\psi_2''(z_2^*)(r^2 - s^2)] + o(N^{-1})$$

Combining equations (80) and (82), we conclude that for  $(x, y) \in \mathfrak{C}$ ,

$$I_{2,2}(4m', 2\xi' + j; 4m, 2\xi + i) = O(N^{-1})$$

where  $i, j \in \{0, 1\}$ . At the beginning of the proof, we assumed  $z_2^* \in [-\beta^2, -\alpha^2]$ . If instead  $z_2^* \in (-\alpha^{-2}, -\beta^{-2}]$ , the procedure would be largely the same as above. The only difference being that we would split up the contour  $\gamma_{w,2}$  as it would be the one that intersects  $\gamma_{s,2}$ .  $\square$

**4.3. Asymptotics of  $I_{2,1}^\alpha$ .** We will now work towards the proof of Proposition 2.1. We begin by manipulating the double contour integral in  $I_{2,1}^\alpha$  into a form that is more amenable to asymptotic analysis. We recall the form of  $I_{2,1}^\alpha$ , which we don't write in terms of the saddle functions presently.

$$(83) \quad \left[ I_{2,1}^\alpha(4m', 2\xi' + j; 4m, 2\xi + i) \right]_{i,j=0}^1 = \frac{1}{(2\pi i)^2} \oint_{\gamma_1} \oint_{\gamma_{0,1}} \frac{dw dz}{z(z-w)} \frac{w^{\xi'+N}(z-1)^N}{z^{\xi+N}(w-1)^N} r_{\alpha,2}(w)^{\frac{N}{2}-m'} \\ \times r_{\alpha,1}(z)^{m-\frac{N}{2}} \frac{2F_{\alpha,2}(w)F_{\beta,1}(w)F_{\alpha,1}(w)}{1+2g_{\alpha,\beta}(w)} F_{\alpha,1}(z)$$

We will repeat a procedure seen in the proof of Corollary 2.1 in Section 3.4. Namely, we will deform the  $w$ -contours through the branch cuts and onto the other sheet of the Riemann surface. In doing so, we gain a single contour integral from the residue at  $z = w$ .

$$(84) \quad \left[ I_{2,1}^\alpha(4m', 2\xi' + j; 4m, 2\xi + i) \right]_{i,j=0}^1 = \frac{1}{(2\pi i)^2} \oint_{\gamma_{Br}} \oint_{\gamma_{0,1}} \frac{dw dz}{z(z-w)} \frac{w^{\xi'+N}(z-1)^N}{z^{\xi+N}(w-1)^N} r_{\alpha,1}(w)^{\frac{N}{2}-m'} \\ \times r_{\alpha,1}(z)^{m-\frac{N}{2}} \frac{2F_{\alpha,1}(w)F_{\beta,2}(w)F_{\alpha,2}(w)}{1+2g_{\alpha,\beta}(w)} F_{\alpha,1}(z) \\ + \frac{1}{2\pi i} \oint_{\gamma_{0,1}} \frac{dz}{z} z^{\xi'-\xi} r_{\alpha,2}(z)^{N-(m+m')} \frac{2F_{\alpha,2}(z)F_{\beta,1}(z)F_{\alpha,1}(z)}{1+2g_{\alpha,\beta}(z)}$$

This leads us to state and prove the following lemma,

**Lemma 4.6.** *For  $m, m', \xi$ , and  $\xi'$  defined by (23) and (24),*

$$(85) \quad \frac{1}{2\pi} \left| \oint_{\gamma_{0,1}} \frac{dz}{z} z^{\xi'-\xi} r_{\alpha,2}(z)^{N-(m+m')} \frac{2F_{\alpha,2}(z)F_{\beta,1}(z)F_{\alpha,1}(z)}{1+2g_{\alpha,\beta}(z)} \right| \leq C e^{-cN}$$

Where  $C$  is some constant matrix and  $c$  is a positive constant.

*Proof.* Using the definitions of  $m, m', \xi$ , and  $\xi'$  from equations (23) and (24) we have,

$$m + m' = 2xN + x_1 + x_2 < N$$

$$\xi' - \xi = y_2 - y_1$$

The single contour integral in equation (84) has no pole at  $z = 1$ , since  $N - (m + m') > 0$ , so we can deform the contour to a circle of radius one centered at the origin,

$$(86) \quad \frac{1}{2\pi i} \oint_{|z|=1} \frac{dz}{z} z^{\xi'-\xi} r_{\alpha,2}(z)^{N-(m+m')} \frac{2F_{\alpha,2}(z)F_{\beta,1}(z)F_{\alpha,1}(z)}{1+2g_{\alpha,\beta}(z)}$$

Along this contour,  $|r_{\alpha,2}(z)| < 1$  and the matrix-valued function

$$\frac{2F_{\alpha,2}(z)F_{\beta,1}(z)F_{\alpha,1}(z)}{1+2g_{\alpha,\beta}(z)}$$

is bounded and analytic, so we can bound the integral accordingly,

$$(87) \quad \frac{1}{2\pi} \left| \oint_{|z|=1} \frac{dz}{z} z^{\xi'-\xi} r_{\alpha,2}(z)^{N-(m+m')} \frac{2F_{\alpha,2}(z)F_{\beta,1}(z)F_{\alpha,1}(z)}{1+2g_{\alpha,\beta}(z)} \right| \leq C |r_{\alpha,2}^{\max}|^{N-(m+m')}$$

where  $r_{\alpha,2}^{\max}$  denotes the maximum value of  $r_{\alpha,2}(z)$  on the unit circle and  $C$  is some constant matrix.  $\square$

To understand the asymptotics of  $I_{2,1}^\alpha$ , we are left considering the asymptotics of the remaining double contour in equation (84). The asymptotics of this double contour integral does depend on the region of the model, so we will consider the asymptotics in the rough and smooth regions separately.

4.3.1. *Asymptotics of  $I_{2,1}^\alpha$  in the Rough Region.* Here we will prove the asymptotics of the double contour integral in equation (84) for  $(x, y) \in \mathfrak{R}$  and  $x < 1/2$ . This result, along with Lemma 4.6, will prove part (1) of Proposition 2.2.

*Proof.* We start by deforming the contours to the contours of steepest descent and ascent detailed in Section 4.1 and Lemma 4.4 and depicted in Figure 11. This deformation produces a single contour integral due to the residue at  $z = w$ , but the contour integral amounts to zero since it contains the matrix product  $F_{\alpha,2}(z)F_{\alpha,1}(z) = 0$ . We are left with the following double contour integral, which we write in terms of the saddle functions.

$$(88) \quad \oint_{\gamma_{R,D}} \oint_{\gamma_{R,A}} \frac{dw dz}{z(z-w)} \frac{w^{\xi'+N}(z-1)^N}{z^{\xi'+N}(w-1)^N} r_{\alpha,1}(w)^{\frac{N}{2}-m'} r_{\alpha,1}(z)^{m-\frac{N}{2}} \frac{2F_{\alpha,1}(w)F_{\beta,2}(w)F_{\alpha,2}(w)}{1+2g_{\alpha,\beta}(w)} F_{\alpha,1}(z)$$

$$= \oint_{\gamma_{R,D}} \oint_{\gamma_{R,A}} \frac{dw dz}{z(z-w)} \frac{2F_{\alpha,1}(w)F_{\beta,2}(w)F_{\alpha,2}(w)}{1+2g_{\alpha,\beta}(w)} F_{\alpha,1}(z)$$

$$\times \exp[N(\psi_1(w; x, y) - \psi_1(z; x, y)) + \varphi_{\alpha,1}(w; x_2, y_2) - \varphi_{\alpha,1}(z; x_1, y_1)]$$

Now we can use saddle point methods to compute the leading order decay of this integral. Since there are two different saddle points, we must consider the contributions from the four combinations.<sup>11</sup> The contributions where different saddle points are used for  $w$  and  $z$  are immediate. We get the leading order term

$$(89) \quad \frac{F_{\alpha,1}(z_l^*)F_{\beta,2}(z_l^*)F_{\alpha,2}(z_l^*)F_{\alpha,1}(z_k^*) \exp \left[ N(\psi_1(z_l^*) - \psi_1(z_k^*)) + \varphi_1(z_l^*) - \varphi_1(z_k^*) + 2i\theta_{lk}(x, y) \right]}{\pi z_k^*(z_k^* - z_l^*)(1+2g_{\alpha,\beta}(z_l^*))N\sqrt{|\psi''(z_k^*)\psi''(z_l^*)|}}$$

where either  $l = 3$  and  $k = 4$  or  $l = 4$  and  $k = 3$ . The function  $\theta_{lk}(x, y)$  depends on the angle of the steepest ascent and descent contours around the saddle points. The term  $\psi_1(z_l^*) - \psi_1(z_k^*)$  is purely imaginary, and thus does not contribute to the decay of the term. The absolute value of the above can be bounded by  $CN^{-1}$ , where  $C$  is some constant matrix.

Now we want to consider the leading order contributions from the terms where we consider  $z$  and  $w$  at the same saddle point. We start by expanding the function  $\psi_1(z)$  around  $z = z_k^*$ ,

$$\psi_1(z) = \psi_1(z_k^*) + \psi_1''(z_k^*)(z - z_k^*)^2 + O((z - z_k^*)^3)$$

In addition, we make the following change of variables,

$$(90) \quad z - z_k^* = sN^{-1/2} \quad w - z_k^* = rN^{-1/2}$$

Combining this gives,

$$(91) \quad N[\psi_1(w) - \psi_1(z)] = \psi_1''(z_k^*)(s^2 - r^2) + O(N^{-1/2})$$

<sup>11</sup>We can let  $w = z_3^*$  or  $w = z_4^*$ . The same applies for  $z$ , thus resulting in four combinations.

We also apply Lemma 4.5 to get,

$$(92) \quad \frac{2F_{\alpha,1}(z)F_{\beta,2}(z)F_{\alpha,2}(z)F_{\alpha,1}(z)}{1+2g_{\alpha,\beta}(z)} = \frac{2F_{\alpha,1}(z_k^*)F_{\beta,2}(z_k^*)F_{\alpha,2}(z_k^*)F'_{\alpha,1}(z_k^*)}{1+2g_{\alpha,\beta}(z_k^*)}N^{-1/2}(s-r) + O(N^{-1})$$

Combining all this we get the leading order asymptotics,

$$(93) \quad \frac{1}{(2\pi)^2} \frac{2F_{\alpha,1}(z_k^*)F_{\beta,2}(z_k^*)F_{\alpha,2}(z_k^*)F'_{\alpha,1}(z_k^*)}{z_k^*(1+2g_{\alpha,\beta}(z_k^*))}N^{-1} \int_{\Gamma_r} \int_{\Gamma_s} \exp[\psi_1''(z_k^*)(s^2-r^2)] ds dr$$

Where  $\Gamma_r$  and  $\Gamma_s$  are lines through the origin whose angles depend on the angle of the contours of steepest descent and ascent, respectively. Combining the results from equations 89, 93 and Lemma 4.6 we obtain the results presented in part (1) of Proposition 2.2.  $\square$

**4.3.2. Asymptotics of  $I_{2,1}^\alpha$  in the Smooth Region.** The results in parts (2) and (3) of Proposition 2.2 are proven using the same procedure as the proof of Proposition 2.1, located in Section 4.2. The main difference we need to address is that  $\psi_1(z)$  has three saddle points on the interval  $[-\alpha^{-2}, -\alpha^2]$ , where  $\psi_2(z)$  only had one. However, Lemma 4.3 gives all the necessary facts needed to repeat the procedure given in Section 4.2. In particular, we are able to deform the contours in the same way described in Section 4.2.

*Proof.* We deform the  $z$ -contour through the central saddle point,  $z_1^*$ , which is a local maximum of  $\text{Re } \psi_1(z)$  along the interval (see Lemma 4.2). We see from Lemma 4.3, that we can utilize the same placement of contours as we did in the proof of Proposition 2.1. Thus, if  $(x, y) \notin \mathfrak{C}$  we can conclude that

$$|I_{2,1}^\alpha(4m', 2\xi' + j; 4m, 2\xi + i)| \leq c_2 e^{-c_1 N}$$

for  $i, j \in \{0, 1\}$  and some positive constants  $c_1$  and  $c_2$ . If  $(x, y) \in \mathfrak{C}$  we have,

$$(94) \quad \left[ I_{2,1}^\alpha(4m', 2\xi' + j; 4m, 2\xi + i) \right]_{i,j=0}^1 = (\pm C_2 \mp \bar{C}_2) \exp[\varphi_{\alpha,2}(z_1^*; x_2 - x_1, y_2 - y_1)] N^{-1} \\ \times \int_{\mathbb{R}} dr \int_{i\mathbb{R}} ds \exp[\psi_2''(z_1^*)(r^2 - s^2)] + o(N^{-1})$$

where

$$(95) \quad C_2 = \frac{2F_{\alpha,2}(z_1^*)F_{\beta,1}(z_1^*)F_{\alpha,1}(z_1^*)F'_{\alpha,2}(z_1^*)}{1+2g_{\alpha,\beta}(z_1^*)}$$

The plus or minus signs in equation (94) depend on whether  $z_1^* > -\alpha^2$  or  $z_1^* < -\alpha^{-2}$ .  $\square$

## 5. AN INTERMEDIATE CORRELATION KERNEL VIA A NON-INTERSECTING PATHS PROCESS

In order to prove the intermediate correlation kernel presented in Lemma 3.1, we must first describe the relationship between the Aztec diamond and the non-intersecting paths process presented in [3]. This explanation can be found in Section 5.1. These results are not new, the bijection was first detailed in [3, Section 5] and then further described in [6]. Once we introduce this process, the formulation of the kernel follows from a slight modification of [3, Theorem 5.2]. This work is done in Section 5.2.

**5.1. Non-Intersecting Paths Process.** Recall the definition of the Aztec diamond graph given by equations (1)-(3). From this definition, we would like to label the four types of edges found in the Aztec diamond graph. We call an edge of the form  $((2j+1, 2k), (2j+2, 2k+1))$  an *east* edge, an edge of the form  $((2j+1, 2k), (2j, 2k+1))$  a *west* edge, an edge of the form  $((2j+1, 2k), (2j+2, 2k-1))$  a *south* edge, and an edge of the form  $((2j+1, 2k), (2j, 2k-1))$  a *north* edge. The different types of edges are depicted in Figure 16.



5.1.1. *The Aztec Diamond to DR Paths.* We will start by relating the Aztec diamond graph to the DR lattice paths model, which was first introduced in [15]. Under an appropriate choice of weighting this model is equivalent to the Aztec diamond. We will explain this bijection here. To start, we will describe the DR graph of size  $n$ . The DR graph of size  $n$  has vertices given by,

$$(96) \quad \mathbf{v}_n^{\text{DR}} = \{(2j, 2k - 1) : 0 \leq j \leq n, 0 \leq k \leq n\}$$

and edges given by,

$$(97) \quad \mathbf{E}_n^{\text{DR}} = \{((2j, 2k - 1), (2j + 2, 2k - 1)) : 0 \leq j \leq n - 1, 0 \leq k \leq n\} \\ \cup \{((2j, 2k - 1), (2j, 2k - 3)) : 0 \leq j \leq n, 1 \leq k \leq n\} \\ \cup \{((2j, 2k - 1), (2j + 2, 2k - 3)) : 0 \leq j \leq n - 1, 1 \leq k \leq n\}$$

An example DR graph is shown in Figure 15. We can draw non-intersecting paths on the DR graph

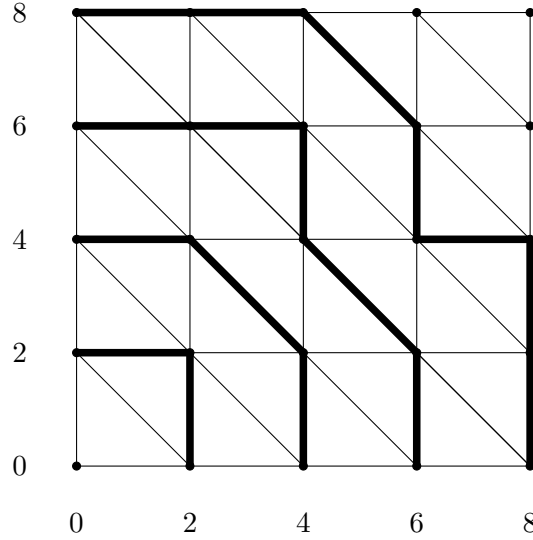


FIGURE 15. The DR graph of size  $n = 4$  with a non-intersecting paths configuration.

that start at the vertices  $\{(0, 2k - 1) : 1 \leq k \leq n\}$  and end at the vertices  $\{(2j, 0) : 1 \leq j \leq n\}$ . Thus the DR graph of size  $n$  has  $n$  non-intersecting paths on it. There is a bijection between coverings of the Aztec diamond and DR paths. Generally speaking, west edges become horizontal edges, east edges become vertical edges, and north edges become diagonal edges. Specifically we write,

- If a dimer covers the edge  $((2j, 2k + 1), (2j + 1, 2k + 2)) \in \mathbf{E}_n^{\text{Az}}$  then the edge  $((2j, 2k + 1), (2j + 2, 2k + 1)) \in \mathbf{E}_n^{\text{DR}}$  is contained in a DR path.
- If a dimer covers the edge  $((2j, 2k + 1), (2j - 1, 2k)) \in \mathbf{E}_n^{\text{Az}}$  then the edge  $((2j, 2k + 1), (2j, 2k - 1)) \in \mathbf{E}_n^{\text{DR}}$  is contained in a DR path.
- If a dimer covers the edge  $((2j, 2k + 1), (2j + 1, 2k)) \in \mathbf{E}_n^{\text{Az}}$  then the edge  $((2j, 2k + 1), (2j + 2, 2k - 1)) \in \mathbf{E}_n^{\text{DR}}$  is contained in a DR path.

If we translate our edge weights in equation (4) to the language of north, south, east and west edges we see that south and west edges always have a weight of 1, while north and east edges can have a weight of 1,  $\varepsilon^2$  or  $\varepsilon^{-2}$ , where  $\varepsilon \in \{\alpha, \beta\}$ . Since south edges are the only ones that do not translate to the DR paths and they always have a weight of 1 in our convention, the edge weights from the Aztec diamond directly translate to edge weights on the DR graph without changing the statistics of the model.

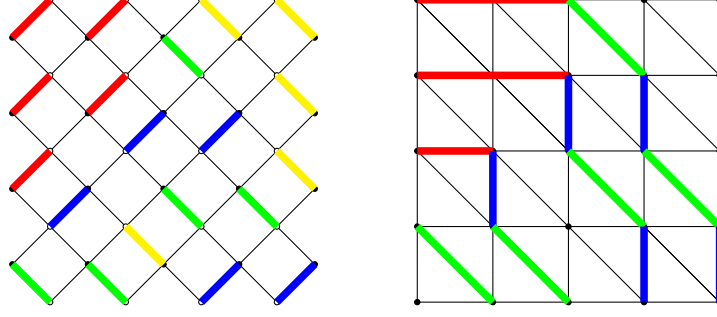


FIGURE 16. On the left is a covering of the Aztec diamond of size  $n = 4$ . East, west, south, and north edges are depicted in blue, red, yellow, and green respectively. The corresponding paths on the DR graph are shown in the figure on the right.

5.1.2. *The Tower Aztec Diamond Graph.* The tower Aztec diamond graph was first described in [3] and later named in [6]. Informally, the  $(n, p)$  tower Aztec diamond graph consists of two Aztec diamonds, one of size  $n$  and the other of size  $n - 1$ , stitched together by a strip of the rotated square grid of length  $p$ . An example of the tower Aztec diamond graph is show in Figure 17. The  $(n, p)$  tower Aztec diamond graph has the vertex sets,

$$(98) \quad W_{n,p}^{\text{Tow}} = \{(2j + 1, 2k) : 0 \leq n - 1, -p - n + 1 \leq k \leq n\}$$

$$(99) \quad B_{n,p}^{\text{Tow}} = \{(2j, 2k + 1) : 0 \leq j \leq n, 0 \leq k \leq n - 1 \text{ or} \\ 0 \leq j \leq n - 1, -p \leq k \leq -1 \text{ or } 1 \leq j \leq n - 1, -p - n \leq k \leq -1 - p\}$$

and edge set give by,

$$(100) \quad E_{n,p}^{\text{Tow}} = \{((2j + 1, 2k), (2j + 2, 2k + 1)) : 0 \leq j \leq n - 1, 0 \leq k \leq n - 1 \text{ or} \\ 0 \leq j \leq n - 2, -p - n + 1 \leq k \leq -1\} \\ \cup \{((2j + 1, 2k), (2j, 2k + 1)) : 0 \leq j \leq n - 1, -p \leq k \leq n - 1 \text{ or} \\ 0 \leq j \leq n - 2, -p - n + 1 \leq k \leq -1 - p\} \\ \cup \{((2j + 1, 2k), (2j + 2, 2k - 1)) : 0 \leq j \leq n - 1, 1 \leq k \leq n \text{ or} \\ 0 \leq j \leq n - 2, 1 - p - n \leq k \leq n\} \\ \cup \{((2j + 1, 2k), (2j, 2k - 1)) : 0 \leq j \leq n - 1, 1 - p \leq k \leq n \text{ or} \\ 1 \leq j \leq n - 1, 1 - p - n \leq k \leq n\}$$

One should realize that it is not possible to have a dimer configuration on the tower Aztec diamond where one dimer contains both a vertex from the corridor and a vertex from either of the appending Aztec diamonds. In fact, there is only one possible dimer configuration on the corridor. Thus the statistics of the tower Aztec diamond can be simplified to the statistics on the two appending Aztec diamond. See [6] for more detail.

5.1.3. *Tower Aztec Diamond to Paths Process.* Just like in the case of the typical Aztec diamond, there is a bijection between the tower Aztec diamond and the tower DR graph, also depicted in Figure 17. The vertices and edges of the tower DR graph are,

$$(101) \quad V_{n,p}^{\text{Tow,DR}} = \{(2j, 2k - 1) : 0 \leq j \leq n, -p \leq k \leq n \text{ or } 1 \leq j \leq n, -p - n + 1 \leq k \leq -p - 1\}$$

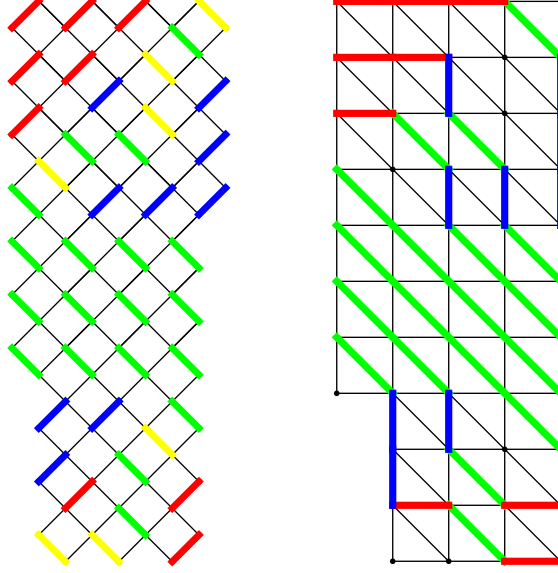


FIGURE 17. A dimer configuration on the  $(4, 3)$  tower Aztec diamond along with the analogous non-intersecting paths configuration on the  $(4, 3)$  tower DR graph.

$$\begin{aligned}
(102) \quad \mathbf{E}_{n,p}^{\text{Tower,DR}} = & \{((2j, 2k - 1), (2j + 2, 2k - 1)) : 0 \leq j \leq n - 1, -p \leq k \leq n\} \\
& \cup \{((2j, 2k - 1), (2j, 2k - 3)) : 0 \leq j \leq n, -p + 1 \leq k \leq n\} \\
& \cup \{((2j, 2k - 1), (2j + 2, 2k - 3)) : 0 \leq j \leq n - 1, -p + 1 \leq k \leq n\} \\
& \cup \{((2j, 2k - 1), (2j + 2, 2k - 1)) : 1 \leq j \leq n - 1, -n - p \leq k \leq -p - 1\} \\
& \cup \{((2j, 2k - 1), (2j, 2k - 3)) : 1 \leq j \leq n, -n - p + 1 \leq k \leq -p - 1\} \\
& \cup \{((2j, 2k - 1), (2j + 2, 2k - 3)) : 1 \leq j \leq n - 1, -n - p + 1 \leq k \leq -p - 1\}
\end{aligned}$$

Once again, we are considering a non-intersecting paths model on the tower DR graph. In this case there are  $n + p$  paths starting at the vertices  $\{(0, 2k - 1) : -p \leq k \leq n\}$  and ending at the vertices  $\{(2n, 2k - 1) : -p - n + 1 \leq k \leq p\}$ . Once again, the weights from the tower Aztec diamond translate directly to the tower DR graph without changing the statistics as long as the south edges have weight one.

The tower DR path process is nearly the process described in [3]. To get exactly the process in their work, we should change the diagonal edges of the DR tower graph into a combination of a horizontal edge and diagonal edge, as depicted in Figure 18. The additional horizontal edges will have weight one and thus not effect the statistics of the model. Once again we consider  $n + p$  non intersection paths which start on the left at the top  $n + p$  vertices and end on the right at the bottom  $n + p$  vertices.

Thus if we send the length of the corridor to infinity, the correlation kernel for the top part of the model, referred to as  $K_{top}$ , in [3]) is also a correlation kernel of the Aztec diamond of size  $n$ . This correlation kernel is stated explicitly in [3, Theorem 3.1].

**5.2. Proof of Lemma 3.1.** Now we have introduced the necessary background to prove Lemma 3.1. We start by defining the matrices

$$(103) \quad \Phi_{\varepsilon,a}(z) = \frac{1}{(1 - a^2 z^{-1})^2} \begin{pmatrix} 1 & \frac{\varepsilon^2}{az} \\ \frac{1}{\varepsilon^2 a} & 1 \end{pmatrix} \begin{pmatrix} 1 & \frac{\varepsilon^2 a}{z} \\ \frac{a}{\varepsilon^2} & 1 \end{pmatrix} \begin{pmatrix} 1 & \frac{1}{az} \\ \frac{1}{a} & 1 \end{pmatrix} \begin{pmatrix} 1 & \frac{a}{z} \\ a & 1 \end{pmatrix}$$

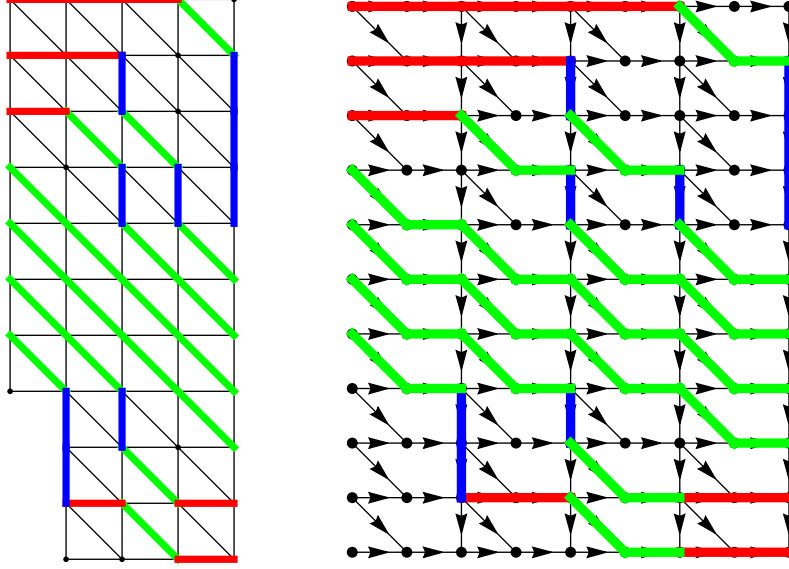


FIGURE 18. The tower DR graph and the equivalent tower graph from the work of Berggren and Duits. The two non-intersecting path configurations are in bijection.

and

$$(104) \quad \phi_{a,N}(z) = \Phi_{\alpha,a}(z)^{\frac{N}{2}} \Phi_{\beta,a}(z)^{\frac{N}{2}}$$

Introducing this parameter  $a$  is necessary in order for us to directly apply [3, Theorem 3.1]. This is because the theorem does not permit singularities on the unit circle. We will call this weighting a split biased two-periodic weighting. Ultimately, we will send  $a \rightarrow 1$  to obtain results for our model of interest. To compute the kernel, we will need to utilize the Weiner-Hopf factorization,

$$(105) \quad \phi_{a,N}(z) = \tilde{\phi}_{-,a,N}(z) \tilde{\phi}_{+,a,N}(z)$$

For a full description of the derivation and properties of the matrices  $\tilde{\phi}_{-,a,N}(z)$  and  $\tilde{\phi}_{+,a,N}(z)$  see [3, Section 3]. It is important to note that  $\tilde{\phi}_{+,a,N}(z)^{\pm 1}$  is analytic for  $|z| < 1$  and continuous for  $|z| \leq 1$ , while  $\tilde{\phi}_{-,a,N}(z)^{\pm 1}$  is analytic for  $|z| > 1$  and continuous for  $|z| \geq 1$ . Moreover, the factorization commutes with the limit  $a \rightarrow 1$ .

The proof of Lemma 3.1 depends on which side of the interface the coordinate  $(4m', 2\xi' + j)$  lies on. We will split this proof into two cases: when  $m' \leq N/2$  and  $m' > N/2$ .

5.2.1. *Proof when  $m' \leq N/2$ .* From [3, Theorem 3.1] we may immediately write the correlation kernel for the split biased two-periodic Aztec diamond.

$$(106) \quad \left[ \mathbb{K}_{a,N}(4m', 2\xi' + j; 4m, 2\xi + i) \right]_{i,j=0}^1 = -\frac{\mathbb{I}_{m > m'}}{2\pi i} \oint_{\gamma_{0,1}} \frac{dz}{z} z^{\xi' - \xi} \Phi_{\alpha,a}(z)^{\frac{N}{2} - m'} \Phi_{\varepsilon,a}(z)^{m - \frac{N}{2}} \\ + \frac{1}{(2\pi i)^2} \oint_{\gamma_a} dw \oint_{\gamma_{0,1,a}} \frac{dz}{z(z-w)} \frac{w^{\xi'}}{z^{\xi}} \Phi_{\alpha,a}(w)^{\frac{N}{2} - m'} \Phi_{\beta,a}(w)^{\frac{N}{2}} \tilde{\phi}_{+,a,N}(w)^{-1} \tilde{\phi}_{-,a,N}(z)^{-1} \phi_{m,a,N}(z)$$

Where

$$(107) \quad \phi_{m,a,N}(z) = \begin{cases} \Phi_{\alpha,a}(z)^m & \text{if } m \leq N/2 \\ \Phi_{\alpha,a}(z)^{\frac{N}{2}} \Phi_{\beta,a}(z)^{m - \frac{N}{2}} & \text{if } m > N/2 \end{cases}$$

The contour  $\gamma_a$  is a simple closed curve around  $a^2$ , while the contour  $\gamma_{0,1,a}$  is a simple closed curve containing 0, 1, and  $\gamma_a$ . To get the correlation kernel for the split two-periodic Aztec diamond, we wish to take the limit as  $a \rightarrow 1$ . The problem is the double contour integral in equation (106) is singular at both  $a^2$  and  $a^{-2}$  (with respect to  $w$ ), and these singularities are converging on opposite sides of the contour  $\gamma_a$  in the limit. We must manipulate the integrand accordingly.

$$(108) \quad \Phi_{\alpha,a}(w)^{\frac{N}{2}-m'} \Phi_{\beta,a}(w)^{\frac{N}{2}} \tilde{\phi}_{+,a,N}(w)^{-1} = \Phi_{\alpha,a}(w)^{-m'} \Phi_{\alpha,a}(w)^{\frac{N}{2}} \Phi_{\beta,a}(w)^{\frac{N}{2}} \tilde{\phi}_{+,a,N}(w)^{-1}$$

$$(109) \quad = \Phi_{\alpha,a}(w)^{-m'} \phi_{a,N}(w) \tilde{\phi}_{+,a,N}(w)^{-1}$$

Now we can apply the eigen-decomposition of  $\phi_{a,N}(w) = \Phi_{\alpha,a}(z)^{\frac{N}{2}} \Phi_{\beta,a}(z)^{\frac{N}{2}}$  to the above. We let  $r_{a,1,N}(w)$  and  $r_{a,2,N}(w)$  denote the eigenvalues of  $\phi_{a,N}(w)$ , which we do not state explicitly here. The key properties of the eigenvalues are stated below. Let  $E_{a,N}(w)$  denote the eigenvector matrix of  $\phi_{a,N}(w)$ , with respect to the above eigenvalue ordering. Then  $F_{a,1,N}(w)$  and  $F_{a,2,N}(w)$  are the following matrices,

$$(110) \quad F_{a,1,N}(w) = E_{a,N}(w) \begin{pmatrix} 1 & 0 \\ 0 & 0 \end{pmatrix} E_{a,N}(w)^{-1}$$

$$(111) \quad F_{a,2,N}(w) = E_{a,N}(w) \begin{pmatrix} 0 & 0 \\ 0 & 1 \end{pmatrix} E_{a,N}(w)^{-1}$$

Using this decomposition, equation (109) becomes,

$$(112) \quad \Phi_{\alpha,a}(w)^{\frac{N}{2}-m'} \Phi_{\beta,a}(w)^{\frac{N}{2}} \tilde{\phi}_{+,a,N}(w)^{-1} = \Phi_{\alpha,a}(w)^{-m'} (r_{a,1,N}(w) F_{a,1,N}(w) + r_{a,2,N}(w) F_{a,2,N}(w)) \tilde{\phi}_{+,a,N}(w)^{-1}$$

The following lemma will be necessary for further simplification and is proven in Section 6.

**Lemma 5.1.** *The eigenvalue  $r_{a,1,N}(w)$  has a pole at  $w = a^2$  and is analytic and non-zero at  $w = a^{-2}$ . The eigenvalue  $r_{a,2,N}(w)$  is analytic and non-zero at  $w = a^2$  and has a zero at  $w = a^{-2}$ . There are no other poles or zeros of the eigenvalue functions in the neighborhood of the contour  $\gamma_a$ .*

We will also need the following statement which is a generalization of Lemma 3.5,

**Lemma 5.2.** *For any  $a \in (0, 1]$ , the matrices  $F_{a,1,N}(w)$  and  $F_{a,2,N}(w)$  are analytic at  $w = a^2$  and  $w = a^{-2}$ .*

This lemma is also proven in Section 6. We can now go back to considering the expression in equation (112). We distribute and consider the two parts of the sum separately. Firstly, note that

$$(113) \quad \Phi_{\alpha,a}(w)^{-m'} r_{a,2,N}(w) F_{a,2,N}(w) \tilde{\phi}_{+,a,N}(w)^{-1}$$

is entirely analytic inside the contour  $\gamma_a$  so, by the residue theorem, this part of the contour integral evaluates to zero. The other part of (112) needs a little massaging,

$$\begin{aligned} \Phi_{\alpha,a}(w)^{-m'} r_{a,1,N}(w) F_{a,1,N}(w) \tilde{\phi}_{+,a,N}(w)^{-1} &= \\ &= \Phi_{\alpha,a}(w)^{-m'} \phi_{a,N}(w) \phi_{a,N}(w)^{-1} r_{a,1,N}(w) F_{a,1,N}(w) \phi_{a,N}(w)^{-1} \tilde{\phi}_{-,a,N}(w) \\ &= \Phi_{\alpha,a}(w)^{\frac{N}{2}-m'} \Phi_{\beta,a}(w)^{\frac{N}{2}} r_{a,1,N}(w)^{-1} F_{a,1,N}(w) \tilde{\phi}_{-,a,N}(w) \end{aligned}$$

All of the parts of the above expression are analytic at  $a^{-2}$ , so we only have poles inside the contour  $\gamma_a$ .<sup>12</sup> Thus, by dominated convergence, we may take the limit  $a \rightarrow 1$ . When  $a = 1$ , we will drop

<sup>12</sup>The matrices  $\Phi_{\varepsilon,a}(w)$ , where  $\varepsilon = \alpha, \beta$ , have poles at  $a^2$  while their inverses have poles at  $a^{-2}$ . The way the expression is written guarantees that these matrices have positive exponents.

the subscript denoting the value of  $a$ . Note that,

$$(114) \quad \tilde{\phi}_-(w) = \frac{1}{(1-w^{-1})^N} \Phi_\alpha(w)^{\frac{N}{2}}$$

by the Weiner-Hopf factorization.<sup>13</sup> Thus the correlation kernel for the split two-periodic Aztec diamond may be written in the following manner in the case where  $0 < m' \leq N/2$ ,

$$(115) \quad \left[ \mathbb{K}_N(4m', 2\xi' + j; 4m, 2\xi + i) \right]_{i,j=0}^1 = -\frac{\mathbb{I}_{m>m'}}{2\pi i} \oint_{\gamma_{0,1}} \frac{dz}{z} z^{\xi'-\xi} \Phi_\alpha(z)^{\frac{N}{2}-m'} \Phi_\varepsilon(z)^{m-\frac{N}{2}} \\ + \frac{1}{(2\pi i)^2} \oint_{\gamma_1} dw \oint_{\gamma_{0,1}} \frac{dz}{z(z-w)} \frac{w^{\xi'+N}(z-1)^N}{z^{\xi+N}(w-1)^N} \Phi_\alpha(w)^{-m'} F_{1,N}(w) \Phi_\alpha(w)^{\frac{N}{2}} \Phi_\varepsilon(z)^{m-\frac{N}{2}}$$

where  $\varepsilon = \alpha$  if  $m \leq N/2$  and  $\varepsilon = \beta$  if  $m > N/2$ .

5.2.2. *Proof when  $m' > N/2$ .* We state the results of [3, Lemma 3.1] under the stated condition,

$$(116) \quad \left[ \mathbb{K}_{a,N}(4m', 2\xi' + j; 4m, 2\xi + i) \right]_{i,j=0}^1 = -\frac{\mathbb{I}_{m>m'}}{2\pi i} \oint_{\gamma_{0,1}} \frac{dz}{z} z^{\xi'-\xi} \Phi_{\alpha,a}(z)^{\frac{N}{2}-m'} \Phi_{\varepsilon,a}(z)^{m-\frac{N}{2}} \\ + \frac{1}{(2\pi i)^2} \oint_{\gamma_a} dw \oint_{\gamma_{0,1,a}} \frac{dz}{z(z-w)} \frac{w^{\xi'}}{z^\xi} \Phi_{\beta,a}(w)^{N-m'} \tilde{\phi}_{+,a,N}(w)^{-1} \tilde{\phi}_{-,a,N}(z)^{-1} \phi_{m,a,N}(z)$$

The double contour integral above has the same issue as the double contour integral in equation (106), the  $w$ -part of the integral has poles at both  $a^2$  and  $a^{-2}$  that we must address before taking the limit.

$$(117) \quad \Phi_{\beta,a}(w)^{N-m'} \phi_{+,a,N}(w)^{-1} = \Phi_{\beta,a}(w)^{\frac{N}{2}-m'} \Phi_{\beta,a}(w)^{\frac{N}{2}} \phi_{+,a,N}(w)^{-1}$$

$$(118) \quad = \Phi_{\beta,a}(w)^{\frac{N}{2}-m'} \Phi_{\alpha,a}(w)^{-\frac{N}{2}} \Phi_{\alpha,a}(w)^{\frac{N}{2}} \Phi_{\beta,a}(w)^{\frac{N}{2}} \phi_{+,a,N}(w)^{-1}$$

The above manipulations have introduced a  $\phi_{a,N}(w) = \Phi_{\alpha,a}(w)^{\frac{N}{2}} \Phi_{\beta,a}(w)^{\frac{N}{2}}$  to the above product, which we replace this with its eigen-decomposition to obtain

$$(119) \quad \Phi_{\beta,a}(w)^{\frac{N}{2}-m'} \Phi_{\alpha,a}(w)^{-\frac{N}{2}} (r_{a,1,N}(w) F_{a,1,N}(w) + r_{a,2,N}(w) F_{a,2,N}(w)) \phi_{+,a,N}(w)^{-1}$$

The expression

$$(120) \quad \Phi_{\beta,a}(w)^{\frac{N}{2}-m'} \Phi_{\alpha,a}(w)^{-\frac{N}{2}} r_{a,2,N}(w) F_{a,2,N}(w) \phi_{+,a,N}(w)^{-1}$$

only has poles outside of the unit circle, and so it contributes nothing to the integral. We are left to manipulate the following,

$$\Phi_{\beta,a}(w)^{\frac{N}{2}-m'} \Phi_{\alpha,a}(w)^{-\frac{N}{2}} r_{a,1,N}(w) F_{a,1,N}(w) \phi_{+,a,N}(w)^{-1}$$

$$(121) \quad = \Phi_{\beta,a}(w)^{N-m'} \phi_{a,N}(w)^{-1} r_{a,1,N}(w) F_{a,1,N}(w) \phi_{a,N}(w)^{-1} \phi_{-,a,N}(w)$$

$$(122) \quad = \Phi_{\beta,a}(w)^{N-m'} r_{a,1,N}(w)^{-1} F_{a,1,N}(w) \phi_{-,a,N}(w)$$

The resulting expression only has poles inside the unit circle, so we are now free to take the limit  $a \rightarrow 1$ . Doing so gives,

$$(123) \quad \left[ \mathbb{K}_N(4m', 2\xi' + j; 4m, 2\xi + i) \right]_{i,j=0}^1 = -\frac{\mathbb{I}_{m>m'}}{2\pi i} \oint_{\gamma_{0,1}} \frac{dz}{z} z^{\xi'-\xi} \Phi_\alpha(z)^{\frac{N}{2}-m'} \Phi_\varepsilon(z)^{m-\frac{N}{2}} \\ + \frac{1}{(2\pi i)^2} \oint_{\gamma_1} dw \oint_{\gamma_{0,1}} \frac{dz}{z(z-w)} \frac{w^{\xi'+N}(z-1)^N}{z^{\xi+N}(w-1)^N} \Phi_\beta(w)^{N-m'} r_{1,N}^{-1}(w) F_{1,N}(w) \Phi_\alpha(w)^{\frac{N}{2}} \Phi_\varepsilon(z)^{m-\frac{N}{2}}$$

<sup>13</sup>See [3, Section 5] for details on how to compute this.

After taking the limit, it will benefit us later to make the following substitution,

$$\begin{aligned}\Phi_\beta(w)^{N-m'} &= \Phi_\beta(w)^{\frac{N}{2}-m'} \Phi_\alpha(w)^{-\frac{N}{2}} \Phi_\alpha(w)^{\frac{N}{2}} \Phi_\beta(w)^{\frac{N}{2}} \\ &= \Phi_\beta(w)^{\frac{N}{2}-m'} \Phi_\alpha(w)^{-\frac{N}{2}} \phi_N(w)\end{aligned}$$

And so the kernel becomes,

$$(124) \quad \mathbb{K}_N(4m', 2\xi' + j; 4m, 2\xi + i) = -\frac{\mathbb{I}_{m>m'}}{2\pi i} \oint_{\gamma_{0,1}} \frac{dz}{z} z^{\xi'-\xi} \Phi_\alpha(z)^{\frac{N}{2}-m'} \Phi_\varepsilon(z)^{m-\frac{N}{2}} \\ + \frac{1}{(2\pi i)^2} \oint_{\gamma_1} dw \oint_{\gamma_{0,1}} \frac{dz}{z(z-w)} \frac{w^{\xi'+N}(z-1)^N}{z^{\xi+N}(w-1)^N} \Phi_\beta(w)^{\frac{N}{2}-m'} \Phi_\alpha(w)^{-\frac{N}{2}} F_{1,N}(w) \Phi_\alpha(w)^{\frac{N}{2}} \Phi_\varepsilon(z)^{m-\frac{N}{2}}$$

## 6. ANALYSIS OF THE EIGEN-DECOMPOSITION

In this section, we take a closer look at the behavior of the eigenvalues and eigenvectors of  $\phi_{a,N}(z)$ . We first prove Lemma 3.6, which appears in the proof of Theorem 2.1 in Section 3. Next, we analyze the poles and zeros of the eigenvalues  $r_{a,1,N}(z)$  and  $r_{a,2,N}(z)$ . In particular, we prove Lemma 5.1. Lastly, we prove Lemma 5.2. Lemmas 5.1 and 5.2 are necessary for the statement of the intermediate correlation kernel in Lemma 3.1. They are also generalizations of Lemmas 3.3 and 3.5, respectively, which both appear in the proof of Theorem 2.1.

**6.1. Proof of Lemma 3.6.** We are immediately ready to prove Lemma 3.6. Recall that we can express  $r_{2,N}(z)$  in terms of the trace of  $\phi_N(z)$ ,

$$r_{2,N}(z) = \frac{1}{2} \left( t_N(z) - \sqrt{t_N(z)^2 - 4} \right)$$

where  $t_N(z) = \text{tr } \phi_N(z)$  is given in equation (33). Fix  $z \in \mathbb{C} \setminus \mathcal{B}$  and choose  $N$  so that  $t_N(z)$  is sufficiently large, we can then expand  $r_{2,N}(z)$  as a series in  $t_N(z)$  around infinity.

$$(125) \quad r_{2,N}(z) = \sum_{k=1}^{\infty} c_k t_N(z)^{1-2k}$$

It is important to note that the coefficients  $c_k$  are independent of  $z$  and  $N$ , however their exact value is not important so we do not explicitly state them. For simplicity, we let  $x = r_{\alpha,1}(z)^{\frac{N}{2}}$  and  $y = r_{\beta,1}(z)^{\frac{N}{2}}$ . We write,

$$(126) \quad t_N(z) = (x^{-1}y + xy^{-1}) \left[ (1/2 + g_{\alpha,\beta}(z))u(x, y) + (1/2 - g_{\alpha,\beta}(z)) \right]$$

where

$$(127) \quad u(x, y) = \frac{xy + x^{-1}y^{-1}}{xy^{-1} + x^{-1}y}$$

For any  $z \in \mathbb{C} \setminus \mathcal{B}$  and  $N$  sufficiently large,  $u(x, y)$  also tends to infinity. So we can write the series expansion of  $t_N(z)^{1-2k}$  in  $u(x, y)$  about infinity,

$$(128) \quad t_N(z)^{1-2k} = (x^{-1}y + xy^{-1})^{1-2k} \sum_{j=2k-1}^{\infty} c'_{k,j} \frac{(1/2 - g_{\alpha,\beta}(z))^{j-2k+1}}{(1/2 + g_{\alpha,\beta}(z))^j} u(x, y)^{-j}$$

where  $c'_{k,j}$  are coefficients independent of  $z$  and  $N$  that we don't state explicitly. We can plug the above into our expansion of  $r_{2,N}(z)$  to get,

$$(129) \quad r_{2,N}(z) = \sum_{k=1}^{\infty} \sum_{j=2k-1}^{\infty} c''_{k,j} \frac{(1/2 - g_{\alpha,\beta}(z))^{j-2k+1}}{(1/2 + g_{\alpha,\beta}(z))^j} \left( \frac{1}{xy + x^{-1}y^{-1}} \right)^j (x^{-1}y + xy^{-1})^{j-2k+1}$$

where  $c''_{k,j} = c_k c'_{k,j}$ . The last piece is simply a Laurent polynomial so we write,

$$(130) \quad (x^{-1}y + xy^{-1})^{j-2k+1} = \sum_{s=0}^{j-2k+1} d_{j,k,s} \left(\frac{y}{x}\right)^{2s-j+2k-1}$$

We also write

$$(131) \quad \left(\frac{1}{xy + x^{-1}y^{-1}}\right)^j = \frac{(xy)^j}{((xy)^2 + 1)^j}$$

and expand in  $xy$  around infinity. Combining these results gives,

$$(132) \quad r_{2,N}(z) = \sum_{k=1}^{\infty} \sum_{j=2k-1}^{\infty} c''_{k,j} \frac{(1/2 - g_{\alpha,\beta}(z))^{j-2k+1}}{(1/2 + g_{\alpha,\beta}(z))^j} \left( \sum_{r=j}^{\infty} d'_{r,j} \left(\frac{1}{xy}\right)^{2r-j} \right) \left( \sum_{s=0}^{j-2k+1} d_{j,k,s} \left(\frac{y}{x}\right)^{2s-j+2k-1} \right)$$

Once again we've introduced the coefficient  $d'_{r,j}$  and  $d''_{j,k,s}$  which are independent of  $z$  and  $N$ . This expansion is convergent as long as  $z \notin \mathcal{B}$  and  $N$  is sufficiently large. Besides  $x$  and  $y$ , the only part of the expansion that depends on  $z$  are the terms

$$\frac{(1/2 - g_{\alpha,\beta}(z))^{j-2k+1}}{(1/2 + g_{\alpha,\beta}(z))^j}$$

It is easy to check that these terms have no pole at  $z = 1$  given the definition of  $g_{\alpha,\beta}(z)$  in equation (14).

We next need to inspect the possible orders of  $x$  and  $y$  that appear in the expansion. Notice that the exponent in the last sum is at most  $j - 2k + 1$  and at least  $-j + 2k - 1$ . Moreover, the smallest exponent in the penultimate sum is  $j$ . Checking the possible powers on  $x$  and  $y$  gives,

$$(133) \quad r_{2,N}(z) = \sum_{p=0}^{\infty} \sum_{q=0}^{\infty} c_{p,q}(z) x^{-(2p+1)} y^{-(2q+1)}$$

The statement in Lemma 3.6 follows from replacing  $x$  and  $y$  with  $r_{\alpha,1}(z)$  and  $r_{\beta,1}(z)$ , respectively.

**6.2. Poles and Zeros of  $r_{a,k,N}(w)$ .** Our ultimate goal in this section is to prove Lemma 5.1. In doing so, we will also prove Lemma 3.3, which is a direct consequence of Lemma 5.1. We begin by stating some equations necessary in defining the eigenvalues  $r_{a,k,N}(w)$ . We start by stating the eigenvalues of  $\Phi_{\varepsilon,a}(w)$ ,

$$(134) \quad r_{a,\varepsilon,1}(w) = \frac{1}{(w-a)^2} \left( (w+1)^2 + \frac{1}{2}w(a+a^{-1})^2(\varepsilon^2 + \varepsilon^{-2}) \right. \\ \left. + (a+a^{-1})(\varepsilon + \varepsilon^{-1})\sqrt{w(w^2 + x_{\varepsilon,a}w + 1)} \right)$$

$$(135) \quad r_{a,\varepsilon,2}(w) = \frac{1}{(w-a)^2} \left( (w+1)^2 + \frac{1}{2}w(a+a^{-1})^2(\varepsilon^2 + \varepsilon^{-2}) \right. \\ \left. - (a+a^{-1})(\varepsilon + \varepsilon^{-1})\sqrt{w(w^2 + x_{\varepsilon,a}w + 1)} \right)$$

where

$$x_{\varepsilon,a} = \frac{1}{4} \left( (a+a^{-1})^2(\varepsilon^2 + \varepsilon^{-2}) - 2(a-a^{-1})^2 \right)$$



The function  $r_{a,\varepsilon,1}(w)$  has a pole at  $w = a^2$  and the function  $r_{a,\varepsilon,2}(w)$  has a zero at  $w = a^{-2}$ . Moreover, these are the only poles and zeros of these functions. These eigenvalues can be used to help compute the eigenvalues of the matrix-valued function  $\phi_{a,N}(w)$ . First we state,

$$(136) \quad \det \Phi_{\varepsilon,a}(w) = \frac{(1 - a^{-2}w^{-1})^2}{(1 - a^2w^{-1})^2}$$

and so

$$(137) \quad \det \phi_{a,N}(w) = \frac{(1 - a^{-2}w^{-1})^{2N}}{(1 - a^2w^{-1})^{2N}}$$

Also,

$$(138) \quad \begin{aligned} \operatorname{tr} \phi_{a,N}(w) = & \left( \frac{1}{2} + g_{a,\alpha,\beta}(w) \right) \left( r_{a,\alpha,1}(w)^{\frac{N}{2}} r_{a,\beta,1}(w)^{\frac{N}{2}} + r_{a,\alpha,2}(w)^{\frac{N}{2}} r_{a,\beta,2}(w)^{\frac{N}{2}} \right) \\ & + \left( \frac{1}{2} - g_{a,\alpha,\beta}(w) \right) \left( r_{a,\alpha,1}(w)^{\frac{N}{2}} r_{a,\beta,2}(w)^{\frac{N}{2}} + r_{a,\alpha,2}(w)^{\frac{N}{2}} r_{a,\beta,1}(w)^{\frac{N}{2}} \right) \end{aligned}$$

where

$$(139) \quad \begin{aligned} g_{a,\alpha,\beta}(w) = & \left( 2a^2(\alpha^2 + \beta^2)(w^2 - 1) + w((\alpha^2 - 1)(\beta^2 - 1)(a^4 + 1) + 2a^2(\alpha^2 + 1)(\beta^2 + 1)) \right) / \\ & \left( 2\sqrt{(a^2 + 1)^2(\alpha^4 + 1)w - 2\alpha^2((a^4 + 1)w - 2a^2(w^2 + w + 1))} \right. \\ & \left. \times \sqrt{(a^2 + 1)^2(\beta^4 + 1)w - 2\beta^2((a^4 + 1)w - 2a^2(w^2 + w + 1))} \right) \end{aligned}$$

Note that these are just the generalized versions of equations (33) and (14). Now we may write the functions  $r_{a,1,N}(w)$  and  $r_{a,2,N}(w)$  in terms of the trace and determinant above,

$$(140) \quad r_{a,1,N}(w) = \frac{1}{2} \left( \operatorname{tr} \phi_{a,N}(w) + \sqrt{(\operatorname{tr} \phi_{a,N}(w))^2 - 4 \det \phi_{a,N}(w)} \right)$$

$$(141) \quad r_{a,2,N}(w) = \frac{1}{2} \left( \operatorname{tr} \phi_{a,N}(w) - \sqrt{(\operatorname{tr} \phi_{a,N}(w))^2 - 4 \det \phi_{a,N}(w)} \right)$$

We are now ready to prove Lemma 5.1.

*Proof.* We will start by justifying that the only potential poles or zeros of the function  $r_{a,k,N}(w)$  with positive real part can occur at the points  $w = a^2$  and  $w = a^{-2}$ . Recall the equation,

$$(142) \quad r_{a,1,N}(w)r_{a,2,N}(w) = \det \phi_{a,N}(w)$$

From this we can deduce that, other than the points  $w = a^2$  and  $w = a^{-2}$ , any pole of  $r_{a,1,N}(w)$  must be a zero of  $r_{a,2,N}(w)$  and vice versa. Additionally, since

$$(143) \quad r_{a,1,N}(w) + r_{a,2,N}(w) = \operatorname{tr} \phi_{a,N}(w)$$

any additional poles or zeros must also be poles of  $\operatorname{tr} \phi_{a,N}(w)$ . Other than  $w = a^2$ , the potential poles of  $\operatorname{tr} \phi_{a,N}(w)$  come from the poles of  $g_{a,\alpha,\beta}(w)$ . These are explicitly,

$$\frac{2(a^2 - 1)^2 \varepsilon^2 - (a^2 + 1)^2 (\varepsilon^4 + 1) \pm (a^2 + 1) (\varepsilon^2 - 1) \sqrt{(a^2 + 1)^2 (\varepsilon^4 + 1) - 2(a^4 - 6a^2 + 1) \varepsilon^2}}{8a^2 \varepsilon^2}$$

For  $\varepsilon = \alpha, \beta$ . One should observe that these values are always negative and real for  $a \in (0, 1]$ . For  $a = 1$ , these are the points  $w = -\varepsilon^2$  and  $w = -\varepsilon^{-2}$ .

Now that we have establish that the only poles or zeros of  $r_{a,1,N}(w)$  and  $r_{a,2,N}(w)$  in the neighborhood of  $\gamma_a$  are at  $w = a^2$  and  $w = a^{-2}$ , we can look specifically at the order of these poles by

considering the Laurent expansions around these points. We start with the following expansions, about  $w = a^2$

$$(144) \quad r_{a,\varepsilon,1}(w) = \frac{c_{a,\varepsilon,+}}{(w - a^2)^2} + O((w - a^2)^{-1})$$

$$(145) \quad r_{a,\varepsilon,2}(w) = d_{a,\varepsilon,+} + O(w - a^2)$$

About  $w = a^{-2}$  we have,

$$(146) \quad r_{a,\varepsilon,1}(w) = c_{a,\varepsilon,-} + O(w - a^{-2})$$

$$(147) \quad r_{a,\varepsilon,2}(w) = d_{a,\varepsilon,-}(w - a^{-2})^2 + O((w - a^{-2})^{-3})$$

The coefficients  $c_{a,\varepsilon,\pm}$  and  $d_{a,\varepsilon,\pm}$  are stated explicitly in Appendix A. We also have the following expansions of the function  $g_{a,\alpha,\beta}(w)$ ,

$$(148) \quad g_{a,\alpha,\beta}(w) = \frac{1}{2} + b_{a,+}(w - a^2) + O((w - a^2)^2)$$

$$(149) \quad g_{a,\alpha,\beta}(w) = \frac{1}{2} + b_{a,-}(w - a^{-2}) + O((w - a^{-2})^2)$$

where coefficients  $b_{a,-}$  and  $b_{a,+}$  are also given in Appendix A. This gives us the information necessary to write the leading order terms of the Laurent expansion of  $\text{tr } \phi_{a,N}(w)$  about  $w = a^2$  and  $w = a^{-2}$

$$(150) \quad \text{tr } \phi_{a,N}(w) = \frac{(c_{a,\alpha,+} + c_{a,\beta,+})^{\frac{N}{2}}}{2(w - a^2)^{2N}} + O((w - a^2)^{-2N+1})$$

$$(151) \quad \text{tr } \phi_{a,N}(w) = \frac{1}{2}(c_{a,\alpha,-} - c_{a,\beta,-})^{\frac{N}{2}} + O(w - a^{-2})$$

Using the above expansions and the form of the determinant, this is enough to see that  $r_{a,1,N}(w)$  has a pole of order  $2N$  at  $w = a^2$  and is analytic and non-zero at  $w = a^{-2}$ . By equation (142), we can conclude that  $r_{a,2,N}(w)$  is analytic and non-zero at  $w = a^2$  and has a zero of order  $2N$  at  $w = a^{-2}$ .  $\square$

**6.3. Analysis of the  $F_N$ -matrices.** For the proofs of Theorem 2.1 and Lemma 3.1 we need to have an understanding of the poles of the matrix valued functions  $F_{a,N,k}(z)$ . In particular, our goal is to prove Lemma 5.2. In turn we will also prove Lemma 3.5, as it is a direct consequence Lemma 5.2. We will avoid explicitly stating the  $F_{a,N}$  matrices as they are quite involved and their form is not insightful.

*Proof.* We write the eigen-decomposition of  $\phi_{a,N}(z)$  as,

$$\phi_{a,N}(z) = E_{a,N}(z)D_{a,N}(z)E_{a,N}(z)^{-1}$$

Where

$$D_{a,N}(z) = \begin{pmatrix} r_{a,1,N}(z) & 0 \\ 0 & r_{a,2,N}(z) \end{pmatrix}$$

And the  $F_{a,N}$  matrices are defined by,

$$F_{a,1,N}(z) = E_{a,N}(z) \begin{pmatrix} 1 & 0 \\ 0 & 0 \end{pmatrix} E_{a,N}(z)^{-1}$$

$$F_{a,2,N}(z) = E_{a,N}(z) \begin{pmatrix} 0 & 0 \\ 0 & 1 \end{pmatrix} E_{a,N}(z)^{-1}$$

First we should note the following equality,

$$(152) \quad F_{a,1,N}(z) + F_{a,2,N}(z) = I$$

Where  $I$  is the identity matrix. This means for any  $z \in \mathbb{C}$ ,  $F_{a,1,N}(z)$  and  $F_{a,2,N}(z)$  must have poles of the same order. We recall some facts about the poles of relevant functions,

	$z = a^2$	$z = a^{-2}$
$r_{a,1,N}(z)$	pole of order $2N$	finite (non-zero)
$r_{a,2,N}(z)$	finite (non-zero)	zero of order $2N$
$\phi_{a,N}(z)$	pole of order $2N$	finite (non-zero)
$\phi_{a,N}(z)^{-1}$	finite (non-zero)	pole of order $2N$

The statements about  $r_{a,1,N}(z)$  and  $r_{a,2,N}(z)$  are proven in Lemma 5.1, while the facts about  $\phi_{a,N}(z)^{\pm 1}$  can be directly computed via the definition in equations (103) and (104). Now we write,

$$(153) \quad \phi_{a,N}(z) = r_{a,1,N}(z)F_{a,1,N}(z) + r_{a,2,N}(z)F_{a,2,N}(z)$$

The order of the pole at  $z = a^2$  must agree on both sides of the equation. Since  $F_{a,1,N}(z)$  and  $F_{a,2,N}(z)$  must have poles of the same order, the only way the equation is consistent is if  $F_{a,1,N}(z)$  and  $F_{a,2,N}(z)$  have no pole at  $z = a^2$ . Similarly, by analyzing the equality

$$(154) \quad \phi_{a,N}(z)^{-1} = r_{a,1,N}(z)^{-1}F_{a,1,N}(z) + r_{a,2,N}(z)^{-1}F_{a,2,N}(z)$$

We can deduce that  $F_{a,1,N}(z)$  and  $F_{a,2,N}(z)$  have no pole at  $z = a^{-2}$ .  $\square$

#### APPENDIX A. EXPLICIT STATEMENT OF COEFFICIENTS

Below we have recorded some coefficients named, but not explicitly stated, in the proof of Lemma 5.1.

$$\begin{aligned}
c_{a,\varepsilon,+} &= \frac{(\varepsilon^2 + 1)^2 (a^2 + 1)^2}{\varepsilon^2} & c_{a,\varepsilon,-} &= \frac{(\varepsilon^2 + 1)^2}{\varepsilon^2 (a^2 - 1)^2} \\
d_{a,\varepsilon,+} &= \frac{\varepsilon^2 (a^2 - 1)^2}{(\varepsilon^2 + 1)^2 a^4} & d_{a,\varepsilon,-} &= \frac{\varepsilon^2 a^4}{(\varepsilon^2 + 1)^2 (a^2 + 1)^2} \\
b_{a,+} &= \frac{(a^4 - 1) (\alpha^2 - \beta^2)^2}{(\alpha^2 + 1)^2 (\beta^2 + 1)^2 (a^3 + a)^2} & b_{a,-} &= -\frac{a^2 (a^2 - 1) (\alpha^2 - \beta^2)^2}{(\alpha^2 + 1)^2 (\beta^2 + 1)^2 (a^2 + 1)}
\end{aligned}$$

#### REFERENCES

- [1] V. Beffara, S. Chhita, and K. Johansson. Airy point process at the liquid-gas boundary. *Ann. Probab.*, 46(5):2973–3013, 2018.
- [2] T. Berggren and A. Borodin. Geometry of the doubly periodic aztec dimer model, 2023.
- [3] T. Berggren and M. Duits. Correlation functions for determinantal processes defined by infinite block Toeplitz minors. *Adv. Math.*, 356:106766, 48, 2019.
- [4] A. Borodin and M. Duits. Biased  $2 \times 2$  periodic aztec diamond and an elliptic curve. *Probab. Theory Relat. Fields*, 187:259–315, 2023.
- [5] C. Boutillier and B. de Tilière. Fock’s dimer model on the aztec diamond, 2024.
- [6] S. Chhita and M. Duits. On the domino shuffling and matrix refactorization. *Commun. Math. Phys*, 401:1417–1467, 2023.
- [7] S. Chhita and K. Johansson. Domino statistics of the two-periodic Aztec diamond. *Adv. Math.*, 294:37–149, 2016.
- [8] S. Chhita, K. Johansson, and B. Young. Asymptotic domino statistics in the Aztec diamond. *Ann. Appl. Probab.*, 25(3):1232–1278, 2015.
- [9] S. Chhita and B. Young. Coupling functions for domino tilings of Aztec diamonds. *Adv. Math.*, 259:173–251, 2014.

- [10] H. Cohn, R. Kenyon, and J. Propp. A variational principle for domino tilings. *J. Amer. Math. Soc.*, 14:297–346, 2001.
- [11] M. Duits and A. B. J. Kuijlaars. The two-periodic Aztec diamond and matrix valued orthogonal polynomials. *J. Eur. Math. Soc. (JEMS)*, 23(4):1075–1131, 2021.
- [12] N. Elkies, G. Kuperberg, M. Larsen, and J. Propp. Alternating-sign matrices and domino tilings I and II. *J. Algebraic Combin.*, 1:111–132, 219–234, 1992.
- [13] B. Eynard and M. Mehta. Matrices coupled in a chain. I. Eigenvalue correlations. *J. Phys. A*, 31:4449–4456, 1998.
- [14] W. Jockush, J. Propp, and P. Shor. Random domino tilings and the arctic circle theorem. *arXiv:math.CO/9801068*, 1998.
- [15] K. Johansson. The arctic circle boundary and the Airy process. *Ann. Probab.*, 33:1–30, 2005.
- [16] P. W. Kasteleyn. The statistics of dimers on a lattice : I. The number of dimer arrangements on a quadratic lattice. *Physica*, 27:1209–1225, 1961.
- [17] R. Kenyon. Lectures on dimers, 2009.
- [18] R. Kenyon, A. Okounkov, and S. Sheffield. Dimers and amoebae. *Ann. of Math.*, 163:1019–1056, 2006.
- [19] A. B. J. Kuijlaars and M. Piorkowski. Wiener-hopf factorizations and matrix-valued orthogonal polynomials, 2024.
- [20] H. N. V. Temperley and M. E. Fisher. Dimer problem in statistical mechanics—an exact result. *Philos. Mag. (8)*, 6:1061–1063, 1961.

DEPARTMENT OF MATHEMATICS, VASSAR COLLEGE, POUGHKEEPSIE NY  
 Email address: mshea@vassar.edu